environmental microbiology

Environmental Microbiology (2021) **23**(6), 3130–3148 doi:10.1111/1462-2920.15536

Sweet spheres: succession and CAZyme expression of marine bacterial communities colonizing a mix of alginate and pectin particles

Carina Bunse,[1,2†] **Hanna Koch**,[3,4†] **Sven Breider**,[3] **Meinhard Simon**[1,3] **and Matthias Wietz**[2,3*]

[1]*Helmholtz Institute for Functional Marine Biodiversity at the University of Oldenburg, Oldenburg, Germany.*

[2]*Alfred Wegener Institute Helmholtz Centre for Polar and Marine Research, Bremerhaven, Germany.*

[3]*Institute for Chemistry and Biology of the Marine Environment, University of Oldenburg, Oldenburg, Germany.*

[4]*Department of Microbiology, Radboud University Nijmegen, Nijmegen, The Netherlands.*

Summary

Polysaccharide particles are important substrates and microhabitats for marine bacteria. However, substrate-specific bacterial dynamics in mixtures of particle types with different polysaccharide composition, as likely occurring in natural habitats, are undescribed. Here, we studied the composition, functional diversity and gene expression of marine bacterial communities colonizing a mix of alginate and pectin particles. Amplicon, metagenome and metatranscriptome sequencing revealed that communities on alginate and pectin particles significantly differed from their free-living counterparts. Unexpectedly, microbial dynamics on alginate and pectin particles were similar, with predominance of amplicon sequence variants (ASVs) from *Tenacibaculum*, *Colwellia*, *Psychrobium* and *Psychromonas*. Corresponding metagenome-assembled genomes (MAGs) expressed diverse alginate lyases, several colocalized in polysaccharide utilization loci. Only a single, low-abundant MAG showed elevated transcript abundances of pectin-degrading enzymes. One specific *Glaciecola* ASV dominated the free-living fraction, possibly persisting on particle-derived oligomers through different glycoside hydrolases. Elevated ammonium uptake and metabolism signified nitrogen as an important factor for degrading carbon-rich particles, whereas elevated methylcitrate and glyoxylate cycles suggested nutrient limitation in surrounding waters. The bacterial preference for alginate, whereas pectin primarily served as colonization scaffold, illuminates substrate-driven dynamics within mixed polysaccharide pools. These insights expand our understanding of bacterial niche specialization and the biological carbon pump in macroalgae-rich habitats.

Received 23 February, 2021; revised 6 April, 2021; accepted 15 April, 2021. *For correspondence. E-mail matthias.wietz@awi.de; Tel. +49-471-48311454; Fax. +49-471-48311776. †These authors contributed equally to this work.

Introduction

Polysaccharides produced by marine macroalgae and phytoplankton are important ecological and biogeochemical agents, serving as structural and storage components for the algae as well as nutrient source for heterotrophic bacteria (Arnosti *et al*., 2021). A considerable fraction of algal polysaccharides is bound in particles, hotspots of microbial activity with central implications for the biological carbon pump (Stocker, 2012). Hydrogels and transparent exopolymer particles (TEP), a subset of polysaccharide particles forming by self-assembly of anionic polysaccharides in seawater, constitute a global amount of ~70 gigatons and are indispensable for the study of particle–microbe interactions (Verdugo *et al*., 2004; Verdugo, 2012; Cordero and Datta, 2016). The building blocks of marine hydrogels largely originate from macroalgae, in which anionic gelling polysaccharides such as alginate can constitute >50% of the biomass (Mabeau and Kloareg, 1987). In addition, phytoplankton produce anionic polymers and contribute to the marine hydrogel pool (Mühlenbruch *et al*., 2018). Natural processes of decay or exudation, such as the release of alginate and rhamnogalacturonan from widespread macroalgae (Koch *et al*., 2019a), presumably result in the formation of hydrogel scaffolds that represent hotspots for microbial life. These events potentially play an ecological role at rocky coasts of temperate seas, which harbor dense forests of macroalgae.

The chemical and structural complexity of marine hydrogels challenges the identification of specific

© 2021 The Authors. *Environmental Microbiology* published by Society for Applied Microbiology and John Wiley & Sons Ltd.
This is an open access article under the terms of the Creative Commons Attribution License, which permits use, distribution and reproduction in any medium, provided the original work is properly cited.

particle–microbe relationships. To reduce this complexity, exposing synthetic model particles to natural bacterioplankton helps understanding the dynamics and drivers of particle colonization. Such approaches have identified hydrogels and other polysaccharide particles as active microbial microhabitats, which harbor distinct communities compared to the surrounding water (Mitulla *et al*., 2016; Sperling *et al*., 2017; Zäncker *et al*., 2019). Furthermore, attached microbes can undergo a temporal succession of primary degraders and opportunistic taxa (Datta *et al*., 2016; Enke *et al*., 2018, 2019). The main indicator of hydrolytic capacities is the presence and diversity of carbohydrate-active enzymes (CAZymes), foremost polysaccharide lyases (PLs) and glycoside hydrolases (GHs), in bacterial genomes (Hehemann *et al*., 2014). CAZymes are commonly clustered in polysaccharide utilization loci (PUL), operon-like regions facilitating efficient hydrolysis (Grondin *et al*., 2017). CAZyme numbers, diversity and genomic organization can distinguish bacteria in primary degraders for initial polymer breakdown, and secondary consumers utilizing oligosaccharides, monosaccharides or other compounds released by primary degraders. These types occur across taxonomic boundaries and also within single species (Hehemann *et al*., 2016; Koch *et al*., 2020).

Nonetheless, it remains enigmatic how bacterial particle utilization proceeds within the natural 'particlescape' – presumably containing a mixture of particle types with different polysaccharide composition – and how these processes are shaped by the taxonomic and functional diversity of the ambient microbiota. The co-availability of hydrogels with different polysaccharide composition might initiate a segregation of bacterial populations by substrate preferences, comparable to hydrolyzing model isolates (Zhu *et al*., 2016; Koch *et al*., 2019a). In this context, the CAZyme repertoire is considered to be a stronger driver of niche specialization than phylogenetic relationships (Hehemann *et al*., 2016; Wolter *et al*., 2021a). The colonization and utilization of particle resources might also include interactions with free-living microbes, which might benefit from oligosaccharides and other compounds released into the surrounding water. In addition, microbial competition and cooperation can coincide with successional patterns and specific interactions (Ebrahimi *et al*., 2019; Gralka *et al*., 2020).

To evaluate particle-specific bacterial dynamics in a mixture of hydrogels, the present study co-exposed alginate and pectin particles to bacterioplankton communities from Helgoland, an island in the southern North Sea surrounded by dense macroalgal forests (Bartsch and Kuhlenkamp, 2000; Uhl *et al*., 2016). Due to the gelling capacities of alginate and pectin and their demonstrated release from Helgoland macroalgae (Koch *et al*., 2019a), we assume that related particles occur in this habitat and constitute microhabitats for specialized microbiota. The co-incubation followed by magnetic separation allowed deciphering community composition, functional potential and gene expression depending on particle type and in relation to the free-living fraction. Opposed to our original hypothesis that alginate and pectin particles are utilized by different members of the ambient community, we observed similar compositional and functional patterns with predominant expression of alginate lyases. The identification of alginate as preferred substrate, whereas pectin primarily served as colonization scaffold, illuminates bacterial microhabitat ecology and substrate cycling in macroalgae-rich habitats with diverse polysaccharide budgets.

Results and discussion

We studied taxonomic diversity, functional capacities and gene expression of particle-attached (PA) marine bacterial communities on alginate (AlgP) and pectin (PecP) particles in comparison to their free-living (FL) counterparts. For this purpose, synthetic AlgP and PecP were co-exposed to bacterioplankton collected near Helgoland Island, surrounded by dense macroalgal forests and hence considerable polysaccharide budgets (Supplementary Fig. 1A). The ambient water was sequentially filtered through 100 and 20 μm before AlgP/PecP addition to exclude naturally occurring particles and larger organisms. For the targeted separation of communities, we then carried out triplicate co-incubations in different combinations of magnetic and non-magnetic particles: (i) magnetic AlgP and non-magnetic PecP, (ii) non-magnetic AlgP and magnetic PecP, and (iii) controls without particles. Applying magnetic force allowed the specific recovery of each particle type (Supplementary Video 1). The FL fraction was obtained by 5 μm filtration to remove non-magnetic particles and collecting the flow-through on 0.2 μm filters (Supplementary Fig. 1B).

Do AlgP, PecP and FL harbour specific communities with temporal variability?

Amplicon sequencing of bacterial 16S rRNA genes revealed significant differences between PA and FL communities (PERMANOVA, $p < 0.001$) but substantial overlap between AlgP and PecP (Fig. 1A, Supplementary Fig. 2A). FL communities from both particle combinations were congruent as expected (Fig. 1A), and FL data were thus combined in subsequent analyses. Furthermore, significant compositional differences of PA and FL communities to those in the ambient seawater and controls without added particles (PERMANOVA, $p < 0.001$) confirmed the observations as true biological dynamics.

© 2021 The Authors. *Environmental Microbiology* published by Society for Applied Microbiology and John Wiley & Sons Ltd.,

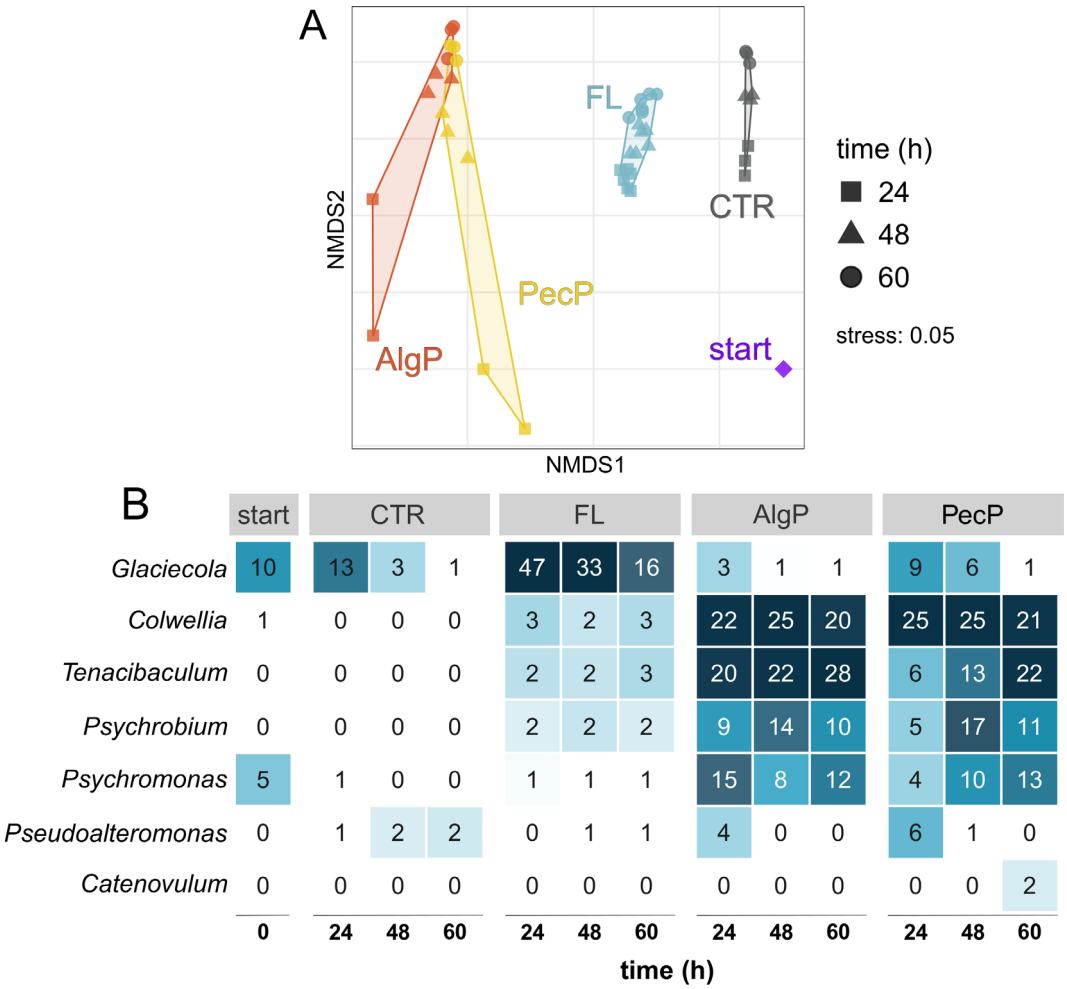

Fig 1. Bacterial community composition based on amplicon sequence variants.
A. Non-metric multidimensional scaling reveals different communities on alginate (AlgP) and pectin particles (PecP) compared to the free-living fraction (FL), control without particles (CTR), and the ambient seawater (start).
B. Relative abundances of dominant genera on AlgP and PecP in comparison to FL, CTR and start communities.

Amplicon sequence variants (ASVs) affiliated with *Tenacibaculum* (*Bacteroidetes*: *Flavobacteriales*), *Colwellia*, *Psychromonas* and *Psychrobium* (*Gammaproteobacteria*: *Alteromonadales*) constituted up to 60% of both AlgP and PecP communities (Fig. 1B), with significant enrichment compared to the FL fraction (Kruskal–Wallis test, $p < 0.001$). Hence, particle colonization largely related to few dominant taxa, comparable to other marine polysaccharide particles (Datta *et al*., 2016; Enke *et al*., 2019). The finding of related strains with considerable CAZyme repertoires on marine macroalgae (Dong *et al*., 2012; Martin *et al*., 2015; Gobet *et al*., 2018; Christiansen *et al*., 2020) supports the ecological relevance of our observations. Notably, both *Colwellia* and *Tenacibaculum* can be enriched on decaying algae (Fernandes *et al*., 2012; Zhu *et al*., 2017) and hence under circumstances when algal polysaccharides might be released and self-assemble into particles. Furthermore, *Tenacibaculum* and *Psychromonas* frequently occur during phytoplankton blooms near Helgoland, when bacterial dynamics are largely driven by algal carbohydrates (Teeling *et al*., 2012; Kappelmann *et al*., 2019; Krüger *et al*., 2019). High adaptability and metabolic rates, illustrated by the rapid stimulation of multiple *Colwellia* ASVs from nearly undetectable levels in the ambient community (Supplementary Fig. 3), could be a competitive advantage during such events.

Glaciecola (*Alteromonadales*) dominated the FL community (Kruskal–Wallis test; $p < 0.0003$), with an average abundance of >30% during the first 48 h with low alpha-diversity (Fig. 1B, Supplementary Fig. 2B). Notably, the *Glaciecola* population was dominated by a single ASV (Supplementary Fig. 3), suggesting that nutrient scarcity in FL favoured highly competitive genotypes. This finding underlined that specific biogeochemical conditions can

© 2021 The Authors. *Environmental Microbiology* published by Society for Applied Microbiology and John Wiley & Sons Ltd.,

stimulate the predominance of single community members (Pedler *et al*., 2014). We hypothesize that *Glaciecola* largely persisted as secondary consumer of particle-derived substrates, supported by genomic evidence from the major corresponding MAG (see below).

The substantial overlap between AlgP and PecP microbiomes contradicted our original hypothesis that the ambient community segregates by particle type. Furthermore, there was little temporal variability in community composition, although we possibly missed rapid successional dynamics as observed in related studies (Datta *et al*., 2016; Enke *et al*., 2019). One exception was *Pseudoalteromonas*, whose sole occurrence at 24 h on both particle types (Fig. 1B; Kruskal–Wallis test, $p = 0.002$) signifies a polysaccharide pioneer (Hehemann *et al*., 2016). This notion is supported by alginolytic and pectinolytic capacities of various *Pseudoalteromonas* species, which generally respond quickly to nutrient input (Ivanova *et al*., 2014; Hehemann *et al*., 2017). The AlgP microbiota established within the first 24 h and then remained unchanged, whereas *Tenacibaculum* established with temporal delay on PecP with peak abundances at 60 h (Fig. 1B; Kruskal–Wallis test, $p = 0.04$). Faster stabilization of the AlgP community indicates that alginate was the major nutrient source, as discussed below in context of metagenomic and metatranscriptomic evidence. One notable exception was *Catenovulum* (*Alteromonadales*), which solely established on PecP after 60 h (Fig. 1B; Kruskal–Wallis test, $p = 0.01$) and was the only taxon linked to pectin degradation (see below).

Do AlgP, PecP and FL communities differ in functional diversity and gene expression?

As taxonomic and metagenomic richness are overall connected (Salazar *et al*., 2019), we expected contrasting functional potentials in PA and FL communities, whereas metabolic capacities of AlgP and PecP communities should be largely congruent. However, AlgP and PecP microbiomes might differ in gene expression patterns, as these can be independent from taxonomic composition (Salazar *et al*., 2019). For instance, certain taxa encode both alginate and pectate lyases (Koch *et al*., 2019a) and might express the corresponding genes differentially depending on particle type. To evaluate these aspects, we analyzed the metagenome (24 and 60 h) and metatranscriptome (60 h) of AlgP and PecP communities in relation to the FL fraction (Supplementary Table 1). This approach included both community-wide and genome-centric perspectives through MAGs.

The metagenomic library of 21 gigabases comprised ~192 000 genes predicted by Prokka, 47% of which were functionally annotated using UniProtKB, KEGG and/or COG databases. Two percent of all genes were predicted to encode CAZymes according to dbCAN2 (Supplementary Table 2). We first assessed overarching differences between PA (i.e. occurring on both AlgP and PecP) and FL communities to identify general signatures of planktonic and attached niches. Transcripts from the citric acid cycle, glycolysis/gluconeogenesis and amino acid metabolism were abundant in both PA and FL metatranscriptomes but numerous pathways differed (Supplementary Table 3). Overall, ~60% of all transcripts were differentially abundant between PA and FL communities (Fig. 2A, Supplementary Table 3), matching metatranscriptomic evidence in other marine ecosystems (Satinsky *et al*., 2014). Transcript abundances of glutamine synthetase, one key enzyme of bacterial nitrogen assimilation converting ammonium into glutamine, peaked in PA communities (Fig. 2B). This observation suggests considerable ammonium uptake to meet the nitrogen demand for fuelling polysaccharide-derived carbon into protein biosynthesis, supported by abundant transcripts of related transporter and regulator genes (Fig. 2B; Wilcoxon rank-sum test, $p < 0.05$). Notably, the biosynthesis of valine, leucine and isoleucine peaked in PA, but their degradation in FL communities (Supplementary Table 3; Wilcoxon rank-sum test, $p < 0.01$). We interpret this observation as provision of amino acids from actively growing PA to substrate-limited FL bacteria. In this context, leucine exchange between bacteria on polysaccharide particles and the surrounding water (Enke *et al*., 2019) might be a stabilizing component of their interactions (Johnson *et al*., 2020). Glyoxylate, dicarboxylate and pyruvate metabolism peaked in FL communities (Supplementary Table 3). Furthermore, induction of the methylcitrate cycle and the glyoxylate shunt (Fig. 2B; Wilcoxon rank-sum test, $p < 0.01$) supports the notion of substrate limitation in the FL niche, matching transcriptomic responses of starved bacterioplankton (Kaberdin *et al*., 2015). These pathways likely promoted persistence by generating energy from short-chain fatty acids but might also alleviate iron limitation or oxidative stress (Palovaara *et al*., 2014; Ahn *et al*., 2016; Dolan *et al*., 2018; Koedooder *et al*., 2018; Serafini *et al*., 2019). In *Alteromonas macleodii*, similar expression patterns were interpreted as maintenance metabolism (van Bodegom, 2007; Beste and McFadden, 2010; Koch *et al*., 2019b).

Next, we specifically compared AlgP and PecP to identify polysaccharide-specific patterns. Communities on AlgP and PecP only slightly differed in functional potential and gene expression (Fig. 2A), compliant with their compositional overlap (Fig. 1). Only 2% of transcripts were differentially abundant, without community-wide patterns

© 2021 The Authors. *Environmental Microbiology* published by Society for Applied Microbiology and John Wiley & Sons Ltd.,

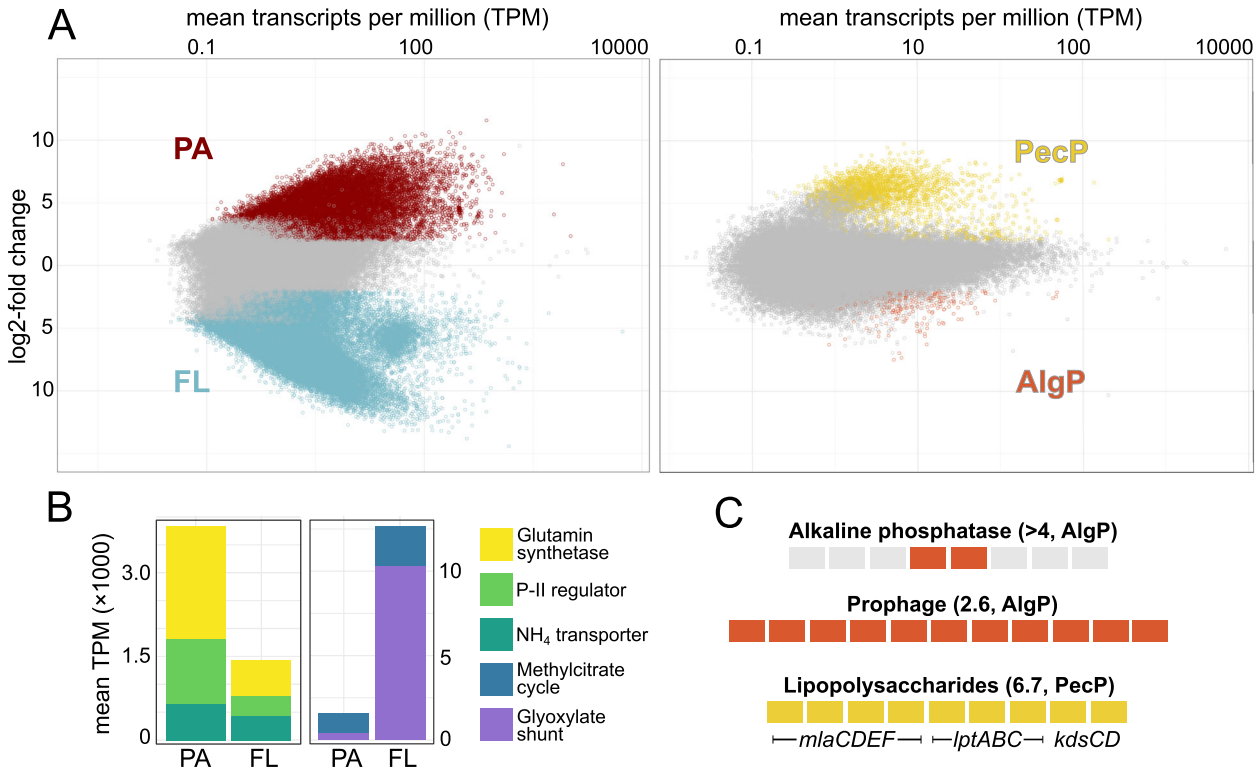

Fig 2. General metagenomic and metatranscriptomic patterns.
A. Differential transcript abundances in PA (both particle types) versus FL (left panel); and in AlgP versus PecP communities (right panel). Coloured dots designate genes with DESEq2 log2-fold changes >2 and $p_{adj} < 0.001$.
B. Selected genes and pathways with higher transcript abundances in PA or FL, including glutamine synthetase (EC number 6.3.1.2) and ammonium transporters (homologs of AmtB (Saier *et al*., 2016)). 'Methylcitrate cycle' is the sum of methyl-isocitrate lyase, methyl-aconitate isomerase, methyl-citrate synthase and aconitate hydratase genes (COG2513, COG2828, COG0372, COG1048). 'Glyoxylate shunt' is the sum of isocitrate lyase and malate synthase genes (EC numbers 4.1.3.1 and 2.3.3.9). P-II regulator: Nitrogen regulatory protein P-II (COG0347). C: Selected gene clusters with higher transcript abundances on AlgP (orange-colored) or PecP (yellow-colored), encoding alkaline phosphatases (locus tags 41274–41275), a predicted prophage (38698–38711) and lipopolysaccharide-related *mla*, *lpt* and *kds* pathways (73039–73048). Values in parentheses designate the mean log2-fold change of genes.

in specific functional categories (Supplementary Table 3). On AlgP, higher transcript abundances of alkaline phosphatase genes possibly counteracted beginning phosphate limitation, comparable to late stages of natural TEP colonization (Berman-Frank *et al*., 2016). Furthermore, higher transcript abundances of predicted prophages (Fig. 2C, Supplementary Table 3) indicates the induction of lytic cycles and corresponding release of organic matter (Breitbart *et al*., 2018). These events potentially stimulated secondary consumers such as *Aureispira*, which only appeared after 60 h (Kruskal–Wallis test, $p = 0.01$). This predatory taxon can feed on metabolic products or cell debris from other bacteria, fuelled by its capacity to adhere to anionic polysaccharides (Furusawa *et al*., 2015). On PecP, a single MAG related to *Catenovulum* accounted for the vast majority of differentially abundant transcripts, supporting the predisposition of this taxon towards pectin (see below). The PecP-specific upregulation of lipopolysaccharide-related *mla*, *lpt* and *kds* genes presumably stimulated biofilm formation, an important advantage for colonization and assimilation of particulate substrates (Sivadon *et al*., 2019).

Community-level diversity and expression of CAZymes

Similarities between AlgP and PecP extended to comparable CAZyme profiles, dominated by PL6 and PL7 alginate lyase genes on both particle types (Supplementary Table 2). PL7 genes for the initial depolymerization of alginate, approximately half including a CBM32 carbohydrate-binding domain, peaked in both copy numbers and transcript abundances (Fig. 3A, Supplementary Table 2). PL15, PL17 and PL18 genes encoding the processing of released oligomers were less numerous but considerably transcribed (e.g. locus tags 183566 and 114168), with the highest transcript abundance of all CAZymes in a PL18 gene (locus tag 127388). The alginate content of >50% in brown macroalgae like

© 2021 The Authors. *Environmental Microbiology* published by Society for Applied Microbiology and John Wiley & Sons Ltd.,

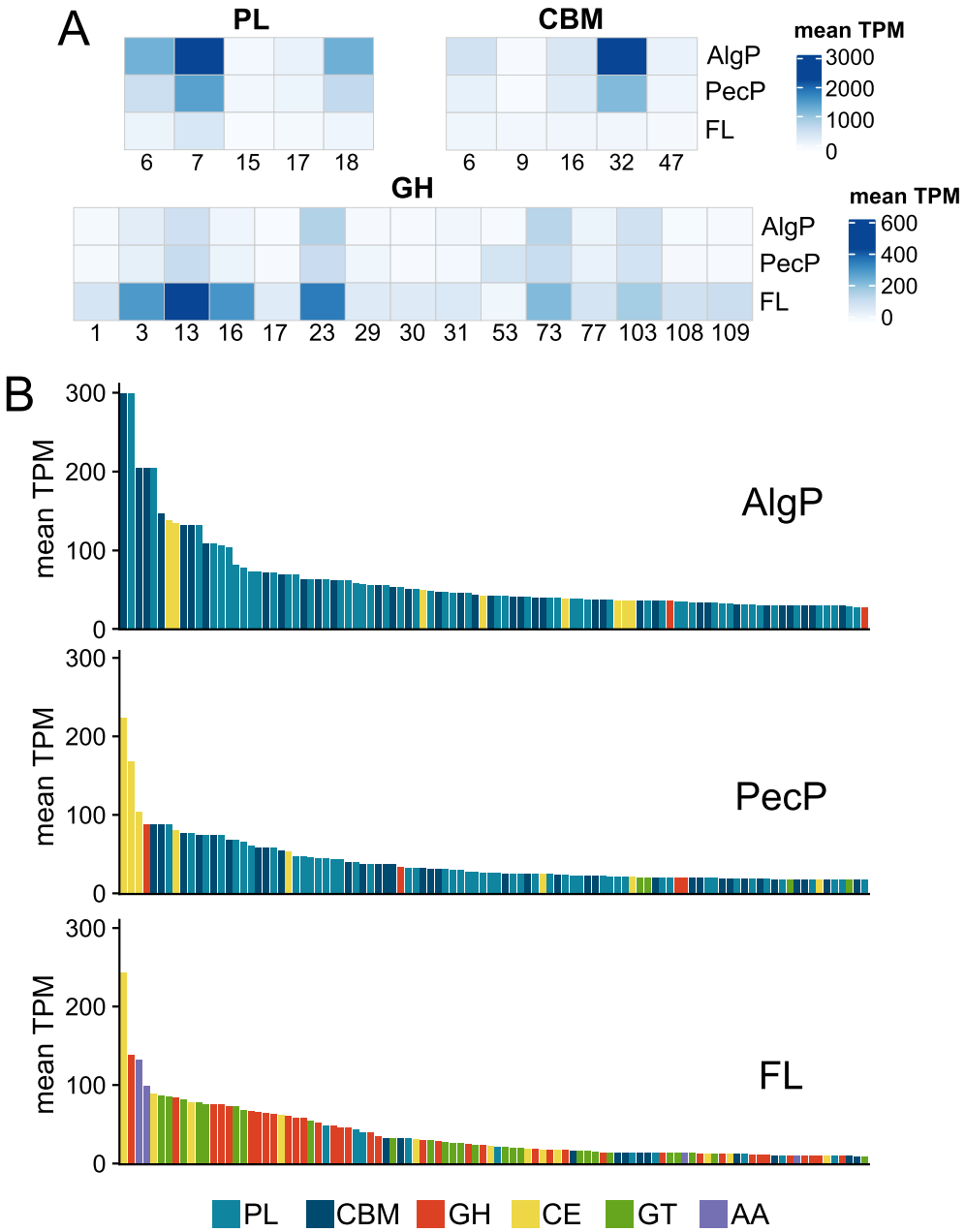

Fig 3. Community-wide diversity and expression of CAZymes.
A. Average transcript abundances of polysaccharide lyases (PL), carbohydrate-binding modules (CBM) and glycoside hydrolases (GH) with mean TPM >50.
B. Top100 CAZymes with the highest expression in the different bacterial fractions.

Saccharina and *Fucus*, which are abundant in our sampling area and release alginate into the water column (Koch *et al*., 2019a), offers an explanation why alginate-degrading genes and organisms predominated. In contrast, we only detected three PL1 pectate lyases and few other pectin-related genes (CE8, GH28, GH105). These results indicate that pectin is not a prime bacterial substrate in kelp forests, although pectinolytic bacteria occur in diverse marine habitats (Van Truong *et al*., 2001; Hehemann *et al*., 2017; Hobbs *et al*., 2019) and pectinous substrates are exuded by Helgoland macroalgae (Koch *et al*., 2019a). Instead, we hypothesise that PecP primarily served as colonization scaffolds for alginolytic bacteria. We propose that the predominant taxa are generally adapted to life on (polysaccharide) particles, favoring cross-particle colonization especially as AlgP were available nearby. The fast sinking of the relatively large particles (diameter ~200 μm) resulted in a loose bottom

© 2021 The Authors. *Environmental Microbiology* published by Society for Applied Microbiology and John Wiley & Sons Ltd.,

layer, with close spatial contact of both particle types. This 'particlescape' potentially allowed cross-particle interactions and utilization of alginate, even if attached to PecP. Nonetheless, significantly higher abundances of alginate lyase transcripts on AlgP (Wilcoxon rank-sum test, $p = 0.0002$ to 10^{-16}) indicates that PecP associates were less alginolytic, possibly attributed to diffusion losses.

The FL community showed a completely different CAZyme signature, with elevated transcript abundances of GHs (Fig. 3A and B). Predominance of families GH3, GH13, GH16 and GH23 (Fig. 3A) matches the hydrolase repertoire of FL bacteria during phytoplankton blooms around Helgoland (Teeling *et al*., 2016; Kappelmann *et al*., 2019). Hence, our observations resemble responses of natural bacterioplankton to oligosaccharide mixtures. Although these GH families are mainly associated with α-1,4-glucan, β-1,3-glucan or peptidoglycan degradation (Lombard *et al*., 2014), our observations indicate a broader range including oligomers of anionic polysaccharides.

CAZymes and PUL on genomic level

Analysis of five near-complete MAGs (>90% completeness at <5% contamination) supported the genomic and ecological differentiation between PA and FL communities (Table 1, Supplementary Table 4). Core-gene phylogeny demonstrated that these MAGs represent the major PA and FL members *Colwellia*, *Tenacibaculum*, *Psychrobium*, *Psychromonas* and *Glaciecola* (Fig. 4A, Supplementary Fig. 4). Accordingly, their normalized coverage matched amplicon-based abundances (Fig. 4B).

Approximately 3% of genes in the major PA-MAGs were annotated as CAZymes (Table 1), mostly PL6, PL7 and PL18 alginate lyases with CBM32, CBM16 or CBM6 domains (Fig. 5). Considerable transcript abundances of alginate lyase and monomer-processing genes *kdgA*, *kdgF*, *kdgK* and *dehR* illustrate the complete metabolization of alginate (Fig. 5, Supplementary Table 4, Supplementary Fig. 5). Approximately half of CAZymes from *Colwellia*, *Psychrobium* and *Psychromonas* MAGs harbour predicted signal peptides (Supplementary Table 4) and were hence likely secreted, although we cannot discern whether these were indeed free enzymes or anchored to the cell membrane. Presumably, CAZyme secretion into the polysaccharide matrix facilitated particle utilization, enhancing polymer hydrolysis and subsequent oligomer uptake (Vetter *et al*., 1998). MAG Gla-32 affiliated with the dominant FL taxon *Glaciecola* encoded only three PLs but 18 GHs, with the highest transcript abundances of families GH3, GH13 and GH23 (Fig. 5). The lower fraction of signal peptides in its CAZymes (30%) indicates that secreted enzymes are less relevant when free-living, pointing towards opportunistic interactions with primary hydrolyzers.

Overall, only some CAZymes of each MAG's repertoire showed elevated transcript abundances (Fig. 5). We assume that the 'silent' CAZymes enable the degradation of other carbohydrates. For instance, the *Colwellia*-MAG Col-24 encodes a homolog of the rarely described PL29 family (locus tag 50313), potentially activated in presence of chondroitin sulfate, dermatan sulfate or hyaluronic acid (Ndeh *et al*., 2018). Although Col-24 clusters with the hydrolytic model isolate *Colwellia echini* A3 (Fig. 4A) at 80% average nucleotide identity (ANI), a BLASTp survey revealed that CAZymes targeting agar, carrageenan and furcellaran are not shared with strain A3 (Supplementary Table 4). Divergent CAZyme repertoires in related *Colwellia* spp. presumably reflect their different habitats (Christiansen *et al*., 2020).

MAG-specific polysaccharide utilization loci. We detected several PUL in the *Tenacibaculum*-MAG Ten-26. For instance, one PUL encodes PL12 and PL17 alginate lyase plus SusCD transporter genes, the hallmark of flavobacterial PUL (Fig. 6A, Supplementary Fig. 6). In contrast, CAZyme genes in gammaproteobacterial MAGs were largely scattered throughout the genomes, although PUL-like operons occur in related taxa (Neumann *et al*., 2015; Schultz-Johansen *et al*., 2018; Christiansen *et al*., 2020). The *Psychromonas*-MAG Psym-73 encodes

Table 1. Characteristics of near-complete metagenome-assembled genomes.

MAG	Taxonomy (GTDB-tk)	Completeness	Contamination	Size (Mbp)	Genes	CAZymes	PLs/GHs
Col-24	*Alteromonadaceae*; *Colwellia*	90	3.0	3.27	2886	91	16/18
Ten-26	*Flavobacteriaceae*; *Tenacibaculum*	97	2.0	3.06	2781	65	17/9
Gla-32	*Alteromonadaceae*; *Glaciecola*	96	0.6	2.77	2575	49	3/18
Psyb-57	*Psychrobiaceae*; *Psychrobium*	95	0.9	2.99	2690	61	16/10
Psym-73	*Psychromonadaceae*; *Psychromonas*	94	1.0	3.69	3337	110	22/34

© 2021 The Authors. *Environmental Microbiology* published by Society for Applied Microbiology and John Wiley & Sons Ltd.,

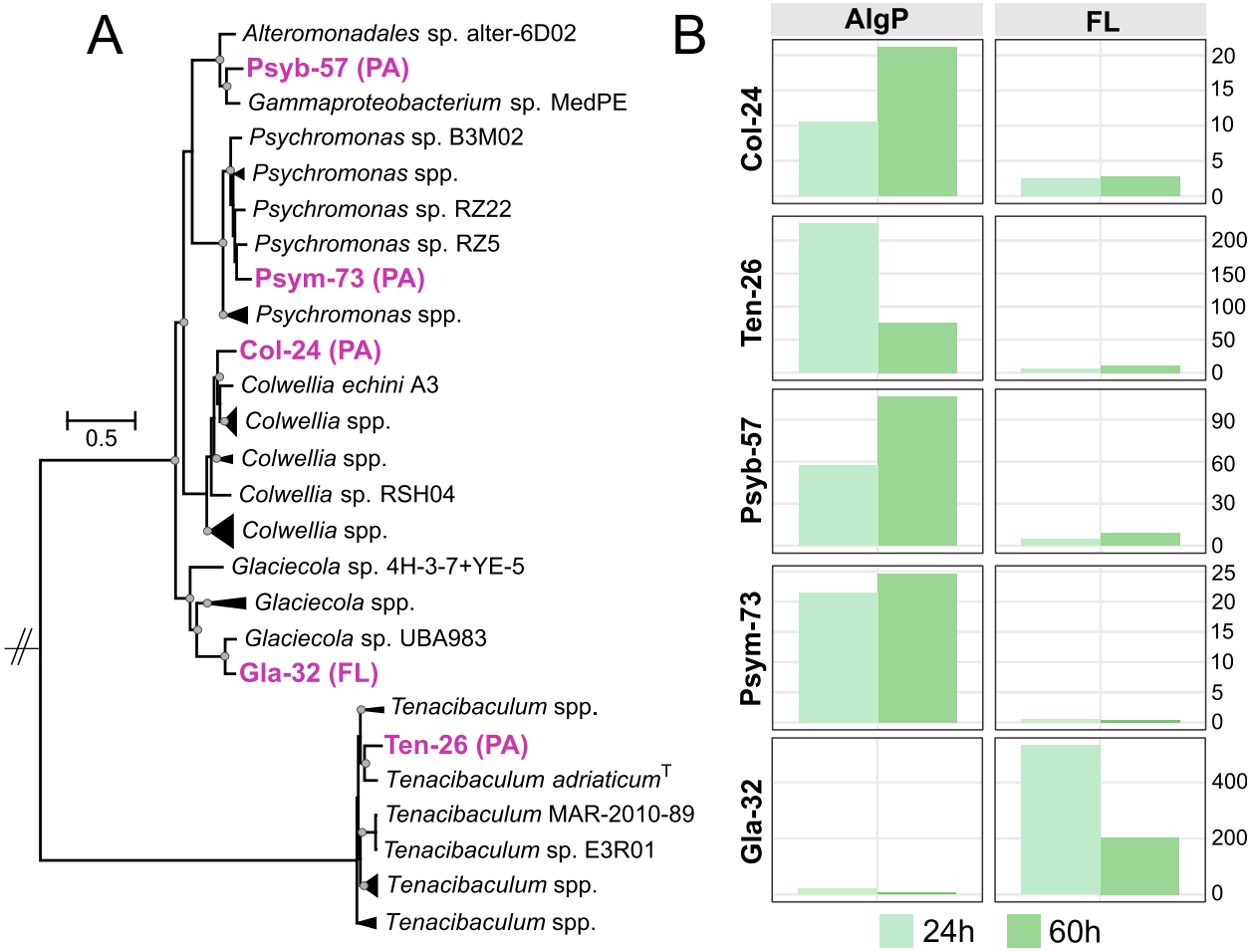

Fig 4. Phylogeny and abundance of metagenome-assembled genomes (MAGs).
A. Maximum-likelihood phylogeny based on 92 single-copy core genes in the context of related genomes. Dots designate nodes with >90% bootstrap support. Supplementary Fig. 4 shows an extended tree including medium-quality MAGs and additional related genomes.
B. Normalized coverage in metagenomes at 24 and 60 h. The scales of *y*-axes differ for better visualization.

two PL7 from subfamilies 5 and 3, each harboring a CBM16 and CBM32 domain (Fig. 6B, Supplementary Table 4). Together with the adjacent CBM16 gene, this combination indicates efficient binding and processing of different alginate architectures (Sim *et al*., 2017; Hu *et al*., 2019). The *Psychrobium*-MAG Psyb-57 encodes a PL12, a candidate novel variant of alginate lyases shared with other bacteria from Helgoland (Kappelmann *et al*., 2019). Colocalization of this PL12 with exopolysaccharide-related genes (Fig. 6C) might link polysaccharide degradation and biosynthesis, considering the regulation of exopolysaccharide metabolism via PLs (Bakkevig *et al*., 2005; Köseoğlu *et al*., 2015). A comparable gene arrangement in an alginolytic *Maribacter* strain from the south Atlantic (Wolter *et al*., 2021b) supports the potential implications for particle colonization.

A GH108 gene unique to *Glaciecola*-MAG Gla-32, colocalized with GH1 and carbohydrate transporter genes (Fig. 6D), might allow scavenging oligomers released from particles. Gla-32 is related to the deep-sea isolate *Glaciecola* sp. 4H-3-7 + YE-5 (Fig. 4A), and their share of 40 CAZymes including a GH13 pair and adjacent GH77 (locus tags 06167–06169) indicates ecological relevance in diverse habitats (Klippel *et al*., 2011). We detected transcripts of PL6 and PL7 lyases as well as the monomer processing pathway in Gla-32 (Fig. 5, Supplementary Table 4), indicating a general ability for alginate depolymerization. However, its incomplete alginate operon compared to known alginate degraders (Supplementary Fig. 7A) might signify inefficient alginolytic activity that limits particle colonization.

Diversity of PL7 homologues in Psym-73. The presence of 14 PL7 genes in the *Psychromonas*-MAG Psym-73 signifies a marked specialization towards alginate, as

© 2021 The Authors. *Environmental Microbiology* published by Society for Applied Microbiology and John Wiley & Sons Ltd.,

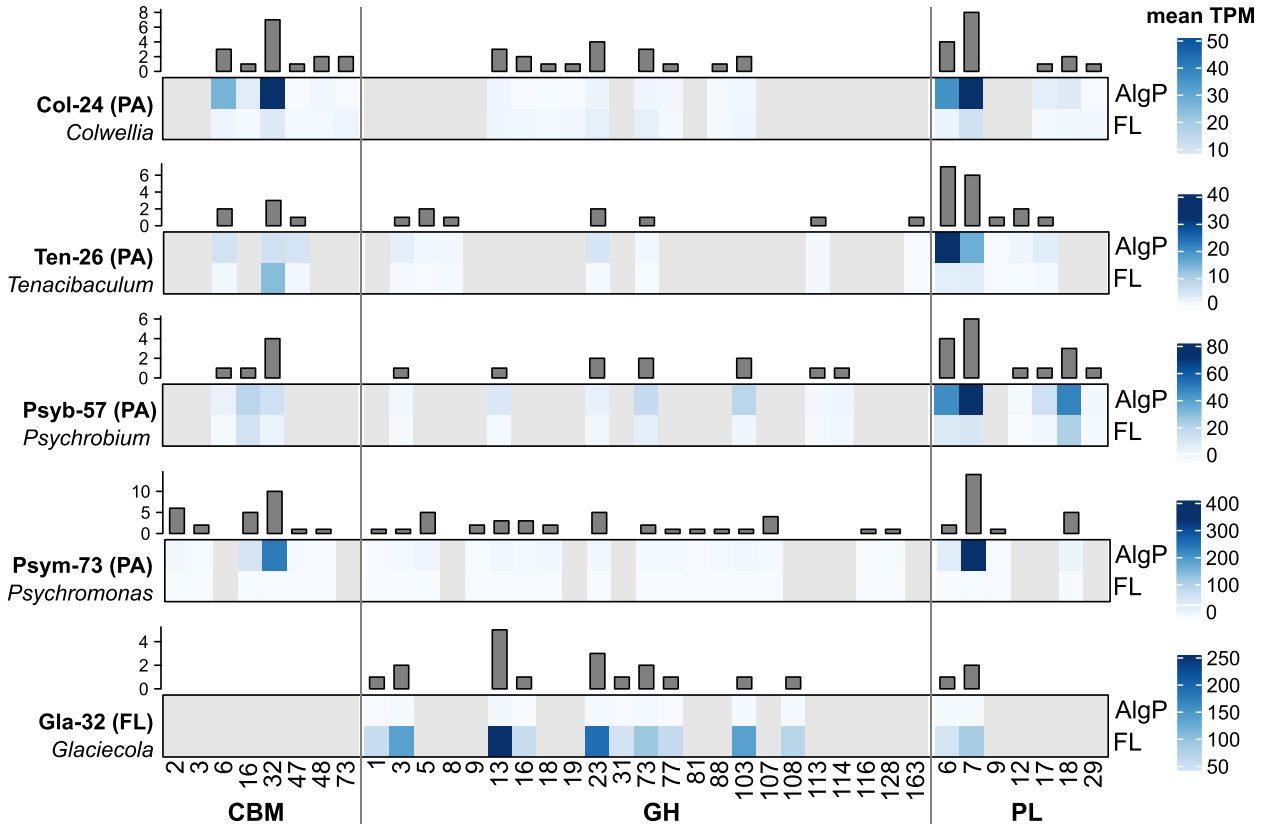

Fig 5. Diversity and expression of CAZymes in metagenome-assembled genomes. Mean transcript abundance (heatmaps) and number (bars) of CAZyme-encoding genes in MAGs affiliated with the dominant PA and FL community members.

hydrolytic activity scales with CAZyme number (Hehemann *et al*., 2016). Two of these homologs (locus tags 20477 and 38641) exhibited the highest transcript abundances of all PL7 genes in our dataset (Supplementary Table 4). Both are related to biochemically characterized lyases from *Vibrio* strains (Supplementary Fig. 8) isolated from macroalgae or seawater (Roux *et al*., 2009; Badur *et al*., 2015; Sun *et al*., 2019). For instance, PL7_38641 has 72% amino acid identity to AlyD of *Vibrio splendidus*, an endolytic lyase releasing three oligomer fractions from guluronate-rich sections (Badur *et al*., 2015). Prediction of a Lipo signal peptide while lacking a CBM indicates that PL7_38641 is anchored as outer membrane lipoprotein (Supplementary Table 4), comparable to AlyA5 from *Zobellia galactanivorans* (Thomas *et al*., 2013).

The two adjacent PL7 genes from different subfamilies (Fig. 6B) possess predicted Sec and Lipo signal peptides respectively (Supplementary Table 4), indicating complementary membrane-bound versus secreted localization to maximize alginate utilization. Homologues of PL7_75913 with >50% amino acid identity also occur in *Simiduia* (*Cellvibrionales*), *Reichenbachiella* and *Marinoscillum* (*Cytophagales*), indicating wide ecological relevance (Spring *et al*., 2015). PL7_75915 from the poorly described subfamily 3 has 55% amino acid identity to a structurally resolved lyase from *Persicobacter* (*Sphingobacteriales*) specialized towards alginate of high molecular weight (Sim *et al*., 2017), suggesting a role in initial depolymerization. We hypothesize that the two PL variants originate from separate horizontal acquisition events with subsequent insertion into the same genomic locus, considering their low similarity and different branching in the phylogenetic tree (Supplementary Fig. 8). Overall, highly variable transcript abundances of PL7 genes (Supplementary Fig. 8) suggest that different variants are activated by specific biochemical conditions, for instance, different alginate characteristics (e.g. polymer length; dissolved or particulate form; or the ratio of mannuronate to guluronate monomers).

Taxa with recurrent occurrence on alginate particles. We compared MAGs Psym-73 and Ten-26 with the genomes of *Psychromonas* sp. B3M02 and *Tenacibaculum* sp. E3R01 respectively; strains isolated in a comparable study on alginate particles (Enke *et al*., 2019). Supported by ~80% ANI and core-gene phylogeny (Fig. 4A), these

© 2021 The Authors. *Environmental Microbiology* published by Society for Applied Microbiology and John Wiley & Sons Ltd.,

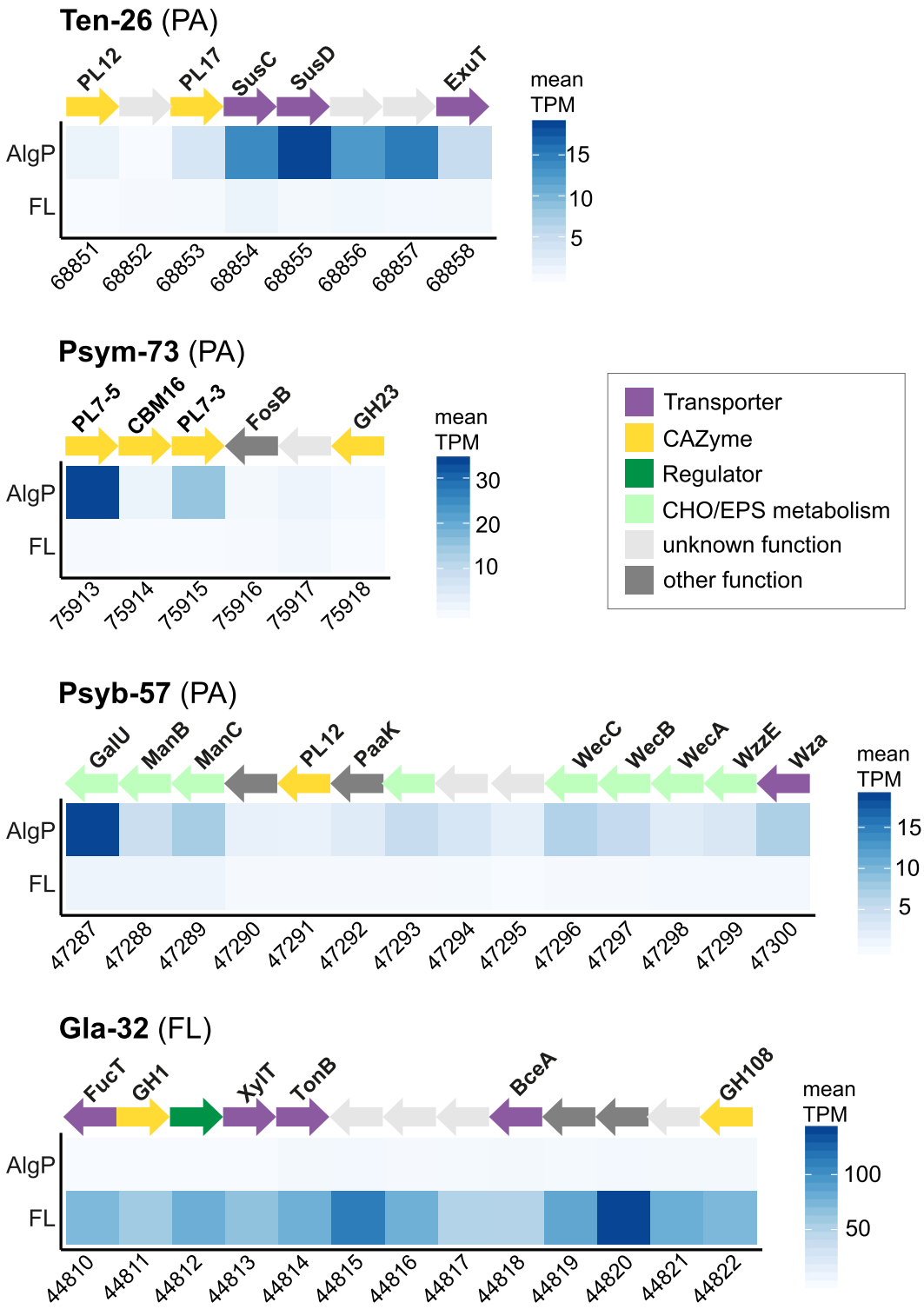

Fig 6. Structure and expression of PUL in MAGs.
A. PUL encoding SusCD and a PL12-PL17 gene pair in *Tenacibaculum*-MAG Ten-26.
B. PL7 genes from different subfamilies colocalized with a CBM16 gene in *Psychromonas*-MAG Psym-73.
C. PL12 and exopolysaccharide-related genes (green) in *Psychrobium*-MAG Psyb-57.
D. Unique GH108 adjacent to GH1 and carbohydrate transporter genes in *Glaciecola*-MAG Gla-32. Supplementary Table 4 and Supplementary Fig. 6 show detailed gene annotations and PUL architectures. EPS: exopolysaccharide; CHO: carbohydrate.

© 2021 The Authors. *Environmental Microbiology* published by Society for Applied Microbiology and John Wiley & Sons Ltd.,

represent related species with presumably wide ecological relevance on polysaccharide particles. Psym-73 and strain B3M02 share nine homologous PLs (Supplementary Table 5), however, encoded in different genomic contexts. This variable organization, together with the higher PL count in Psym-73, indicates considerable CAZyme diversity and genomic rearrangements among hydrolytic *Psychromonas*. Ten-26 and strain E3R01 share 29 homologous CAZymes. However, no PLs were detected in E3R01 while Ten-26 encodes 17 (Supplementary Table 5). These observations indicate CAZyme-related niche specialization among *Tenacibaculum* species, consistent with CAZyme variability in *Tenacibaculum* type strains ranging from eight PLs in *T. jejuense* to none in *T. mesophilum* (Lombard *et al*., 2014).

A single, rare pectin degrader. Despite the compelling evidence that alginate was the preferred bacterial substrate, MAG21 is a candidate for pectin utilization. MAG21 accounted for ~95% of differentially abundant transcripts on PecP (Fig. 7A), contributing to significantly elevated GH abundances and normalized coverage compared to AlgP (Fig. 7B, Kruskal–Wallis test, $p < 10^{-16}$). MAG21 encodes several genes for galacturonate degradation and processing of pectin monomers. A GH53 endo-galactanase gene with the fourth-highest transcript abundance of all CAZymes on PecP (locus tag 118003) might cleave galacturonate-rich side chains from pectinous substrates by endolytic activity (Benoit *et al*., 2012). Moreover, colocalized GH53 and GH2 plus two carbohydrate transporter genes (Fig. 7B) resemble a galacturonan-related PUL in *Bacteroides thetaiotaomicron* (Luis *et al*., 2018). Thus, MAG21 might utilize oligomeric side chains of pectin, processing the resulting galacturonate via tagaturonate and altronate to 2-keto-3-deoxy-D-gluconate through UxuABC (Supplementary Table 4, Supplementary Fig. 5). Genome-based taxonomy assigned MAG21 to the uncultured taxon GCA-2401725, whereas the majority of CAZymes possess homologs in *Catenovulum* spp. (Supplementary Table 4), recently described for pectinolytic capacities (Furusawa *et al*., 2021). Growth of the *Catenovulum* isolate CCB-QB4 on unsaturated galacturonate has been linked to GH28 and GH105 enzymes, which are also encoded by MAG21 (Supplementary Table 4). Together with the restriction of *Catenovulum* ASVs to PecP (Fig. 1C) we propose that MAG21 is taxonomically and functionally related to *Catenovulum* and degrades galacturonate. The medium quality of MAG21 (76% estimated completeness) may explain why pectate lyases are missing compared to CCB-QB4. Alternatively, MAG21 indeed only encodes an incomplete degradation cascade, only accessing oligomeric side chains or oligomers released by the activity of primary degraders that encode pectate lyases.

An additional PecP-specific pattern occurred in *Psychromonas*-MAG Psym-73, with significantly higher transcript abundances of a hybrid gene cluster for the biosynthesis of a siderophore as well as spermidine (Supplementary Table 3, Supplementary Fig. 7B). Homologues of the siderophore-encoding section have been identified in diverse marine bacteria with shown iron-chelating activity (Koch *et al*., 2019b), indicating a similar functionality in Psym-73. The upstream spermidine-related section has ~40% amino acid similarity to the polyamine synthesis pathway of *Vibrio*, indicating a PecP-specific role in biofilm formation (Lee *et al*., 2009).

Ecological conclusions

The predominance of alginolytic pathways demonstrates alginate particles as preferred microbial substrate, whereas pectin was primarily a colonization scaffold. The establishment of similar communities contradicted our original hypothesis of community segregation by substrate preferences. On the contrary, the expression of alginate lyases when attached to pectin signify the concept of a 'particlescape' encompassing cross-particle interactions. Such a scenario might resemble natural processes when algal polysaccharide exudates enter the water column, self-assemble into particles and sink to the seafloor. Under such circumstances, bacteria might utilize alginate even if attached to neighboring microhabitats, e.g. by secreting extracellular CAZymes or exploiting hydrolytic activity of co-occurring microbes. The predominance of few taxa indicates that polysaccharide availability stimulates only certain community members, outcompeting most other strains by their extensive CAZyme repertoire. Nonetheless, identification of a single MAG with pectin-specific dynamics suggests that numerically rare but competitive bacteria can establish in specific niches. Single-particle incubations and the application of ^{13}C-labelled substrates followed by NanoSIMS or stable isotope probing might answer these open questions in future studies. Altogether, our study illuminates central elements of the biological carbon pump in macroalgae-rich habitats, with implications for microscale ecology, niche specialization and bacteria–algae interactions.

Experimental procedures

Characteristics of polysaccharide particles

Custom polysaccharide particles consisting of alginate (CAS #9005-38-3) or pectin (CAS #9000-69-5), approximately 200 μm in diameter, were fabricated by geniaLab

© 2021 The Authors. *Environmental Microbiology* published by Society for Applied Microbiology and John Wiley & Sons Ltd.,

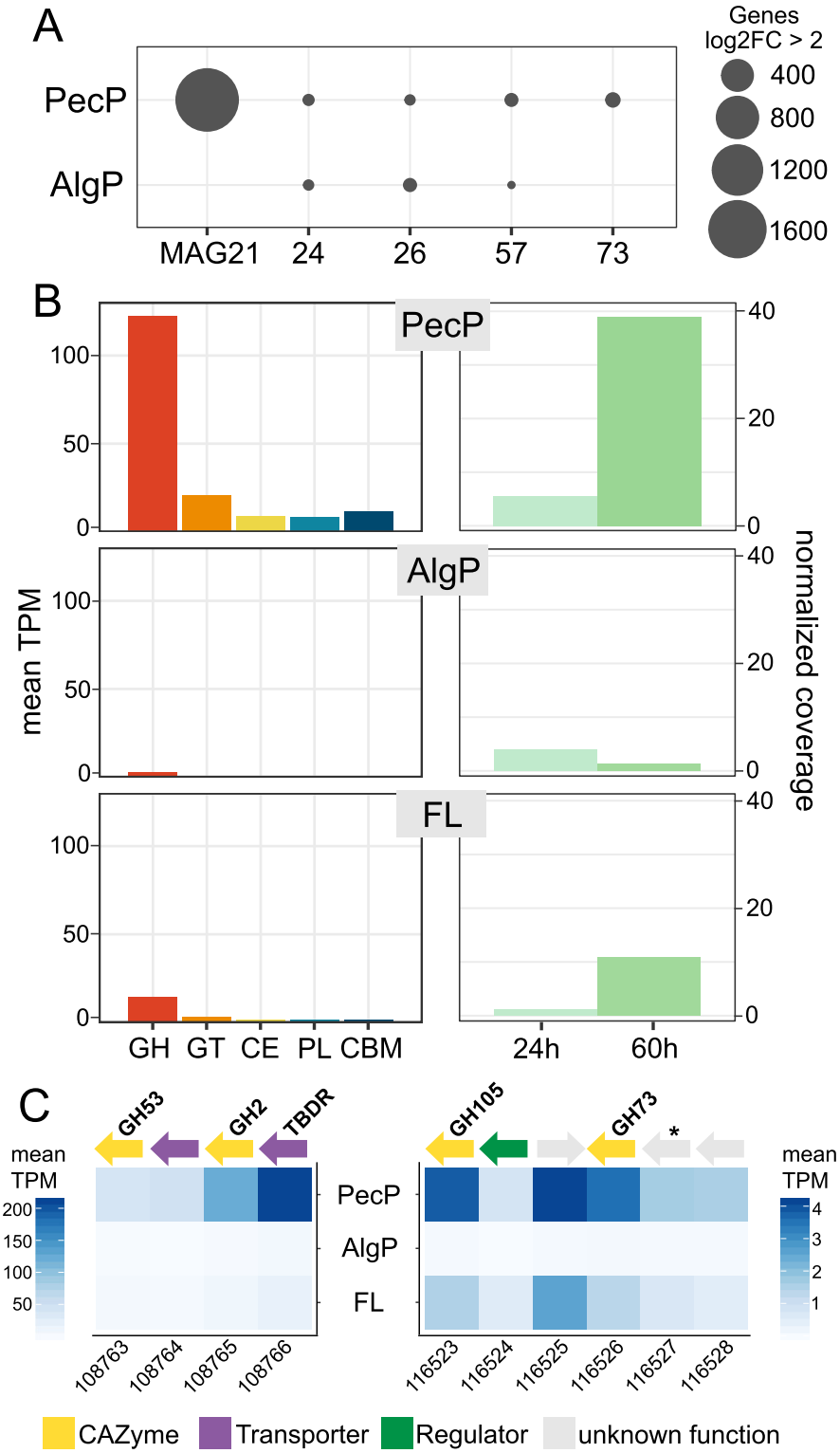

Fig 7. MAG21 as candidate for pectin degradation.
A. Numbers of differentially abundant transcripts compared to the major PA-MAGs on PecP versus AlgP.
B. Elevated transcript abundances of glycoside hydrolase genes on PecP. C, left panel: PUL with similarities to the pectinolytic operon BT4667–4673 in *Bacteroides thetaiotaomicron*. C, right panel: PUL encoding GH105 and GH73 genes plus a hypothetical protein with 60% amino acid identity to an alpha-amylase from *Paraglaciecola arctica* (UniProtKB accession K6ZD77; indicated by asterisk).

© 2021 The Authors. *Environmental Microbiology* published by Society for Applied Microbiology and John Wiley & Sons Ltd.,

(Braunschweig, Germany) by immersing polysaccharide in calcium chloride solution containing metallic beads (Supplementary Methods). Four different versions were produced: magnetic alginate and pectin particles (polysaccharide coated on magnetite core) as well as non-magnetic alginate and pectin particles (polysaccharide coated on ferrous iron core). Particles contained on average 4% polysaccharide (Supplementary Table 6), approximating the 1:100 solid:solvent ratio in natural hydrogels (Verdugo *et al*., 2004). Magnetic and non-magnetic particles of each polysaccharide allowed co-incubation of both polysaccharides and hence similar selection pressures per treatment (i.e. always two available particle types, only varying in magnetism). Applying external magnetic force (Supplementary File 1) subsequently allowed the targeted sampling of particle types.

Seawater sampling and experimental set-up

Seawater was sampled from approx. 1 m depth above macroalgal forests at Helgoland Island (54.190556 N, 7.866667 E) in June 2017. Seawater was filtered through a 100 μm mesh, brought to the lab within 2 h, and filtered again through a 20 μm mesh to remove larger particles and organisms. Each 12 L of filtered seawater were distributed into 20 L Clearboy bottles (Nalgene, Rochester, NY) previously rinsed with the same seawater. Per bottle, 10 μM $NaNO_3$ and 1 μM NaH_2PO_4 (wt./vol.) were added as additional nitrogen and phosphorous source to avoid limitation. Three experiments were set up in triplicate: (i) magnetic alginate particles and non-magnetic pectin particles, (ii) non-magnetic alginate particles and magnetic pectin particles, and (iii) control without particles (Supplementary Fig. 1). Each particle type was added at 3500 L^{-1}, resulting in ~42 000 particles per bottle. Bottles were incubated statically at 15°C (approx. *in situ* temperature) in the dark.

Sampling and nucleic acid extraction of particle-associated and free-living cells

250 ml of the original seawater were filtered onto 0.2 μm polycarbonate filters for determination of the ambient *in situ* community (start). Filters were flash-frozen in liquid nitrogen and stored at −80°C. Incubations were sampled after 24, 48 and 60 h. At each sampling point, bottles were mixed by inversion and ca. 550 ml withdrawn into rinsed measuring cylinders. Each sample was distributed (2 × 250 ml) into sterile RNase-free Nunc tubes (cat. no. 376814; Thermo Fisher Scientific, Waltham, MA). Particle-associated communities on magnetic AlgP or PecP were sampled by holding a neodymium magnet (cat. no. Q-40-10-10-N; Supermagnete, Gottmadingen, Germany) next to the tube. AlgP and PecP were washed with sterile seawater (filtered through 100 and 20 μm; mixed 3:1 with ddH_2O to prevent salt precipitation during autoclavation for 20 min at 121°C) and transferred to 2 ml RNase-free microcentrifuge tubes. The supernatant was transferred to a separate tube and non-magnetic particles were removed by filtration through 5 μm polycarbonate filters. The flow-through was captured on 0.2 μm polycarbonate filters to obtain the FL community. All samples were directly flash-frozen in liquid nitrogen and stored at −80°C. Simultaneous extraction of DNA and RNA was done using a modification of Schneider *et al*. (2017). Purified DNA and RNA were sent on dry ice to DNASense (Aalborg, Denmark) for quality control and sequencing. For particles, several subsamples per replicate were pooled to obtain sufficient DNA and RNA (Supplementary Table 1).

16S rRNA gene amplicon sequencing

Briefly, the V3–V4 region of bacterial 16S rRNA genes was sequenced using primers 341F-806R (Sundberg *et al*., 2013) with MiSeq technology (Illumina, San Diego, CA). Internal company standards worked as expected (Supplementary Methods). Reads were classified into ASVs using DADA2 (Callahan *et al*., 2016) and taxonomically assigned using SILVA v132 (Quast *et al*., 2013). Rarefaction analysis showed that diversity was reasonably covered (Supplementary Fig. 9). Replicates were congruent per treatment and time, without significant differences in Bray–Curtis dissimilarities (PERMANOVA; $p = 0.72$ to 0.98). Furthermore, FL communities from AlgP and PecP were congruent as expected, and FL data combined in subsequent analyses. Alpha-diversity indices (richness, Shannon and inverse Simpson) were calculated using R package iNEXT (Hsieh *et al*., 2016).

Metagenomics

As amplicon data confirmed the consistency of replicates, DNA from the three AlgP, PecP and FL replicates at 24 and 60 h were pooled respectively. DNA was quantified using Qubit (Thermo Fisher Scientific) and fragmented to ~550 bp using M220 using microTUBE AFA fibre screw tubes (Covaris, Woburn, MA) for 45 s at 20°C with duty factor 20%, peak/displayed power 50 W, and cycles/burst 200. Libraries were prepared using the NEB Next Ultra II kit (New England Biotech, Ipswich, MA) and paired-end sequenced (2 × 150 bp) on a NextSeq system (Illumina). Adaptors were removed using cutadapt v1.10 (Martin, 2011) and reads assembled using SPAdes v3.7.1 (Bankevich *et al*., 2012). Genes were predicted using Prokka (Seemann, 2014) and assigned to KEGG categories using KAAS-SBH-GhostX (Moriya *et al*., 2007). CAZymes were predicted using dbCAN2

© 2021 The Authors. *Environmental Microbiology* published by Society for Applied Microbiology and John Wiley & Sons Ltd.,

with CAZyDB v8 (Zhang *et al*., 2018), only considering hits with >80% coverage. Ammonium transporters were predicted by BLASTp of AmtB (P69681) in the Transporter Classification Database (Saier *et al*., 2016).

Metatranscriptomics

RNA was quantified in duplicate per sample using the Qubit BR RNA assay (Thermo Fisher Scientific). RNA quality and integrity were confirmed using TapeStation with RNA ScreenTape (Agilent, Santa Clara, CA). rRNA was depleted using the Ribo-Zero Magnetic kit (Illumina) and residual DNA removed using the DNase MAX kit (Qiagen, Hilden, Germany). Following sample cleaning and concentrating using the RNeasy MinElute Cleanup kit (Qiagen), rRNA removal was confirmed using TapeStation HS RNA ScreenTapes (Agilent). Sequencing libraries were prepared using the TruSeq Stranded Total RNA kit (Illumina), quantified using the Qubit HS DNA assay (Thermo Fisher Scientific) and size-estimated using TapeStation D1000 ScreenTapes (Agilent). For RNA from particle samples, four to five subsamples per replicate were pooled in equimolar concentrations and sequenced on a HiSeq2500 in a 1 $\times$ 50 bp Rapid Run (Illumina). As the first sequencing run did not deliver sufficient data for seven metatranscriptomes, a second run was performed on the same library. PCA confirmed consistent sequencing runs (data not shown), and read counts were subsequently aggregated. Raw fastq sequence reads were trimmed using USEARCH v10.0.2132 (Edgar, 2010) using -fastq_filter and settings -fastq_minlen 45 -fastq_truncqual 20. rRNA reads were removed using BBDuk (http://jgi.doe.gov/data-and-tools/bb-tools) using the SILVA database as reference (Quast *et al*., 2013). Reads were mapped to the predicted genes using Minimap2, discarding reads with sequence identities <0.98. Relative transcript abundances were obtained by dividing raw counts by the length of each gene (RPK) and normalized by per-million scaling factors. Resulting transcripts per million (TPM) were summed per gene annotation (Supplementary Table 2). Differential transcript abundances were calculated on raw read counts using the default DESeq2 workflow in R v3.6 (Love *et al*., 2014; R Core Team, 2018) in RStudio (https://rstudio.com), only considering log2-fold changes >2 with $p_{adj} < 0.001$ (Supplementary Table 3).

MAG binning and analysis

MAGs were binned using MetaBat2 and mmgenome2 (Karst *et al*., 2016; Kang *et al*., 2019). Reads were mapped back to the assembly using Minimap2 v2.5 (Li, 2018), and the average coverage of each bin was calculated using mmgenome2 (weighted by scaffold sizes). Based on results from CheckM and GTDB-Tk (Parks *et al*., 2015; Chaumeil *et al*., 2020), we selected five near-complete MAGs (≥90% estimated genome completeness and <5% genome contamination) representing the major taxa in amplicon data (Table 1, Supplementary Table 4). Whole-genome comparison with type strains was carried out using the MiGA web application (Rodriguez-R *et al*., 2018). Normalized coverage in metagenomic data was calculated following Poghosyan *et al*. (2020) after multiplying the coverage of each MAG in every sample with a normalization factor (sequencing depth of the largest sample divided by the sequencing depth of each individual sample). A maximum-likelihood phylogeny based on 92 core genes identified using the UBCG pipeline (Na *et al*., 2018), including medium-quality MAGs (>70% estimated completeness/<10% contamination) assigned to the same genus plus related genomes from public databases, was calculated using RaxMLHPC-Hybrid v8.2.12 with the GTRGAMMA substitution model and 1000 bootstrap replicates on the CIPRES Science Gateway v3.3 (Miller *et al*., 2010; Stamatakis, 2014). Genes were assigned to KEGG categories using KAAS, and pathways reconstructed from these predictions using KEGG Pathway Mapper (Moriya *et al*., 2007; Kanehisa and Sato, 2020). Gene annotations were refined using UniProtKB/Swiss-Prot (Boutet *et al*., 2016) by custom-BLAST in Geneious v7 (https://www.geneious.com). Genes for processing alginate and pectin monomers were predicted based on the fully reconstructed pathways in *A. macleodii* and *Gramella forsetii* (Kabisch *et al*., 2014; Koch *et al*., 2019a). For comparative purposes, CAZymes of strains B3M02 and E3R01 (Enke *et al*., 2019) were re-annotated with dbCAN2 v8.0 and compared to MAGs Ten-26 and Psym-73 using custom-BLAST in Geneious, only considering hits with >30% query coverage and >40% amino acid identity. ANIs between genomes were calculated using enveomics (Rodriguez-R and Konstantinidis, 2016). Prophages and biosynthetic gene clusters were predicted using PHASTER and antiSMASH 5.0 respectively (Arndt *et al*., 2016; Blin *et al*., 2019). Amino acid sequences of PL7 genes from Psym-73 were aligned using the MAFFT E-INS-i algorithm with default parameters (Katoh *et al*., 2002). A maximum-likelihood phylogeny with 500 bootstrap replicates was calculated using RaxML v8.0 (Stamatakis, 2014) and the WAG+G + F substitution model determined using ModelTest-NG (Darriba *et al*., 2020), both run on CIPRES (Miller *et al*., 2010).

Data availability

All sequencing data have been deposited at NCBI under BioProject PRJEB38771 (see Supplementary Table 1 for accession numbers of each sequence file). Annotated

© 2021 The Authors. *Environmental Microbiology* published by Society for Applied Microbiology and John Wiley & Sons Ltd.,

metagenome contigs and near-complete MAGs, genes and translations, metatranscriptomic counts and the DNA–RNA extraction protocol are available at https://doi.org/10.5281/zenodo.4171148. Rscripts and additional input files for reproducing the analysis are available at https://github.com/matthiaswietz/sweet-spheres. Major R packages used for analysis and visualization included phyloseq, ampvis2, tidyverse, ComplexHeatmap, gtools and PNWColors (McMurdie and Holmes, 2013; Gu *et al*., 2016; Andersen *et al*., 2018; Wickham *et al*., 2019; Lawlor, 2020; Warnes *et al*., 2020).

Acknowledgements

We are indebted to Antje Wichels, Eva-Maria Brodte, Gunnar Gerdts and Uwe Nettelmann (Biological Department Helgoland) for exceptional scientific and logistic support during the experimental work. Mara Heinrichs, Felix Milke and Mathias Wolterink are gratefully acknowledged for excellent technical assistance. Many thanks to geniaLab (Braunschweig), in particular Ulli Jahnz, for their exceptional service and helpful discussions in the preparation of custom polysaccharide particles. Sequencing was carried out by DNASense (Aalborg), with professional support by Mads Albertsen, Thomas Yssing Michaelsen, Rasmus H. Kirkegaard and Martin Hjorth Andersen. We thank Jan-Hendrik Hehemann, Silvia Vidal-Melgosa and Agata Mystkowska for valuable discussions. C.B. was supported by HIFMB, a collaboration between the Alfred Wegener Institute Helmholtz Centre for Polar and Marine Research and the Carl-von-Ossietzky University Oldenburg, initially funded by the Ministry for Science and Culture of Lower Saxony and the Volkswagen Foundation through the 'Niedersächsisches Vorab' program (grant number ZN3285). H.K. was supported by Volkswagen Foundation under VW-Vorab grant 'Marine Biodiversity across Scales' (MarBAS; ZN3112) and by the Netherlands Organization for Scientific Research (NWO Talent Programme grant VI.Veni.192.086). M.W. was supported by grant WI3888/1-2 from the German Research Foundation.

References

Ahn, S., Jung, J., Jang, I.-A., Madsen, E.L., and Park, W. (2016) Role of glyoxylate shunt in oxidative stress response. *J Biol Chem* **291**: 11928–11938.

Andersen, K.S.S., Kirkegaard, R.H., Karst, S.M., and Albertsen, M. (2018) ampvis2: an R package to analyse and visualise 16S rRNA amplicon data. *bioRxiv* **299537**.

Arndt, D., Grant, J.R., Marcu, A., Sajed, T., Pon, A., Liang, Y., and Wishart, D.S. (2016) PHASTER: a better, faster version of the PHAST phage search tool. *Nucleic Acids Res* **44**: W16–W21.

Arnosti, C., Wietz, M., Brinkhoff, T., Hehemann, J.-H., Probandt, D., Zeugner, L., and Amann, R. (2021) The biogeochemistry of marine polysaccharides: sources, inventories, and bacterial drivers of the carbohydrate cycle. *Ann Rev Mar Sci* **13**: 81–108.

Badur, A.H., Jagtap, S.S., Yalamanchili, G., Lee, J.-K., Zhao, H., and Rao, C.V. (2015) Alginate lyases from alginate-degrading *Vibrio splendidus* 12B01 are endolytic. *Appl Environ Microbiol* **81**: 1865–1873.

Bakkevig, K., Sletta, H., Gimmestad, M., Aune, R., Ertesvåg, H., Degnes, K., *et al*. (2005) Role of the *Pseudomonas fluorescens* alginate lyase (AlgL) in clearing the periplasm of alginates not exported to the extracellular environment. *J Bacteriol* **187**: 8375–8384.

Bankevich, A., Nurk, S., Antipov, D., Gurevich, A.A., Dvorkin, M., Kulikov, A.S., *et al*. (2012) SPAdes: a new genome assembly algorithm and its applications to single-cell sequencing. *J Comput Biol* **19**: 455–477.

Bartsch, I., and Kuhlenkamp, R. (2000) The marine macroalgae of Helgoland (North Sea): an annotated list of records between 1845 and 1999. *Helgol Mar Res* **54**: 160–189.

Benoit, I., Coutinho, P.M., Schols, H.A., Gerlach, J.P., Henrissat, B., and de Vries, R.P. (2012) Degradation of different pectins by fungi: correlations and contrasts between the pectinolytic enzyme sets identified in genomes and the growth on pectins of different origin. *BMC Genomics* **13**: 321.

Berman-Frank, I., Spungin, D., Rahav, E., Van Wambeke, F., Turk-Kubo, K., and Moutin, T. (2016) Dynamics of transparent exopolymer particles (TEP) during the VAHINE mesocosm experiment in the new Caledonian lagoon. *Biogeosciences* **13**: 3793–3805.

Beste, D.J.V., and McFadden, J. (2010) System-level strategies for studying the metabolism of *Mycobacterium tuberculosis*. *Mol Biosyst* **6**: 2363–2372.

Blin, K., Shaw, S., Steinke, K., Villebro, R., Ziemert, N., Lee, S.Y., *et al*. (2019) antiSMASH 5.0: updates to the secondary metabolite genome mining pipeline. *Nucleic Acids Res* **47**: W81–W87.

Boutet, E., Lieberherr, D., Tognolli, M., Schneider, M., Bansal, P., Bridge, A.J., *et al*. (2016) UniProtKB/Swiss-Prot, the manually annotated section of the UniProt KnowledgeBase: how to use the entry view. *Methods Mol Biol*: **1374**, 23–54.

Breitbart, M., Bonnain, C., Malki, K., and Sawaya, N.A. (2018) Phage puppet masters of the marine microbial realm. *Nat Microbiol* **3**: 754–766.

Callahan, B.J., McMurdie, P.J., Rosen, M.J., Han, A.W., Johnson, A.J.A., and Holmes, S.P. (2016) DADA2: high-resolution sample inference from Illumina amplicon data. *Nat Methods* **13**: 581–583.

Chaumeil, P.-A., Mussig, A.J., Hugenholtz, P., and Parks, D.H. (2020) GTDB-Tk: a toolkit to classify genomes with the genome taxonomy database. *Bioinformatics* **36**: 1925–1927.

Christiansen, L., Pathiraja, D., Bech, P.K., Schultz-Johansen, M., Hennessy, R., Teze, D., *et al*. (2020) A multifunctional polysaccharide utilization gene cluster in *Colwellia echini* encodes enzymes for the complete degradation of κ-carrageenan, ι-carrageenan, and hybrid β/-κ-carrageenan. *mSphere* **5**: e00792-19.

Cordero, O.X., and Datta, M.S. (2016) Microbial interactions and community assembly at microscales. *Curr Opin Microbiol* **31**: 227–234.

Core Team, R. (2018) *R: A Language and Environment for Statistical Computing*. Vienna, Austria: R Foundation for Statistical Computing.

© 2021 The Authors. *Environmental Microbiology* published by Society for Applied Microbiology and John Wiley & Sons Ltd.,

Darriba, D., Posada, D., Kozlov, A.M., Stamatakis, A., Morel, B., and Flouri, T. (2020) ModelTest-NG: a new and scalable tool for the selection of DNA and protein evolutionary models. *Mol Biol Evol* **37**: 291–294.

Datta, M.S., Sliwerska, E., Gore, J., Polz, M.F., and Cordero, O.X. (2016) Microbial interactions lead to rapid micro-scale successions on model marine particles. *Nat Commun* **7**: 11965.

Dolan, S.K., Wijaya, A., Geddis, S.M., Spring, D.R., Silva-Rocha, R., and Welch, M. (2018) Loving the poison: the methylcitrate cycle and bacterial pathogenesis. *Microbiology* **164**: 251–259.

Dong, S., Yang, J., Zhang, X.-Y., Shi, M., Song, X.-Y., Chen, X.-L., and Zhang, Y.-Z. (2012) Cultivable alginate Lyase-excreting bacteria associated with the Arctic brown alga *Laminaria*. *Mar Drugs* **10**: 2481–2491.

Ebrahimi, A., Schwartzman, J., and Cordero, O.X. (2019) Cooperation and spatial self-organization determine rate and efficiency of particulate organic matter degradation in marine bacteria. *Proc Natl Acad Sci U S A* **116**: 23309–23316.

Edgar, R.C. (2010) Search and clustering orders of magnitude faster than BLAST. *Bioinformatics* **26**: 2460–2461.

Enke, T.N., Datta, M.S., Schwartzman, J., Cermak, N., Schmitz, D., Barrere, J., *et al*. (2019) Modular assembly of polysaccharide-degrading marine microbial communities. *Curr Biol* **29**: 1528–1535.e6.

Enke, T.N., Leventhal, G.E., Metzger, M., Saavedra, J.T., and Cordero, O.X. (2018) Microscale ecology regulates particulate organic matter turnover in model marine microbial communities. *Nat Commun* **9**: 2743.

Fernandes, N., Steinberg, P., Rusch, D., Kjelleberg, S., and Thomas, T. (2012) Community structure and functional gene profile of bacteria on healthy and diseased thalli of the red seaweed *Delisea pulchra*. *PLoS One* **7**: e50854.

Furusawa, G., Azami, N.A., and Teh, A.-H. (2021) Genes for degradation and utilization of uronic acid-containing polysaccharides of a marine bacterium *Catenovulum* sp. CCB-QB4. *PeerJ* **9**: e10929.

Furusawa, G., Hartzell, P.L., and Navaratnam, V. (2015) Calcium is required for ixotrophy of *Aureispira* sp. CCB-QB1. *Microbiology* **161**: 1933–1941.

Gobet, A., Mest, L., Perennou, M., Dittami, S.M., Caralp, C., Coulombet, C., *et al*. (2018) Seasonal and algal diet-driven patterns of the digestive microbiota of the European abalone *Haliotis tuberculata*, a generalist marine herbivore. *Microbiome* **6**: 60.

Gralka, M., Szabo, R., Stocker, R., and Cordero, O.X. (2020) Trophic interactions and the drivers of microbial community assembly. *Curr Biol* **30**: R1176–R1188.

Grondin, J.M., Tamura, K., Déjean, G., Abbott, D.W., and Brumer, H. (2017) Polysaccharide Utilization Loci: fuelling microbial communities. *J Bacteriol* **199**: e00860-16.

Gu, Z., Eils, R., and Schlesner, M. (2016) Complex heatmaps reveal patterns and correlations in multidimensional genomic data. *Bioinformatics* **32**: 2847–2849.

Hehemann, J.-H., Arevalo, P., Datta, M.S., Yu, X., Corzett, C.H., Henschel, A., *et al*. (2016) Adaptive radiation by waves of gene transfer leads to fine-scale resource partitioning in marine microbes. *Nat Commun* **7**: 12860.

Hehemann, J.-H., Boraston, A.B., and Czjzek, M. (2014) A sweet new wave: structures and mechanisms of enzymes that digest polysaccharides from marine algae. *Curr Opin Struct Biol* **28**: 77–86.

Hehemann, J.-H., Truong, L.V., Unfried, F., Welsch, N., Kabisch, J., Heiden, S.E., *et al*. (2017) Aquatic adaptation of a laterally acquired pectin degradation pathway in marine gammaproteobacteria. *Environ Microbiol* **19**: 2320–2333.

Hobbs, J.K., Hettle, A.G., Vickers, C., and Boraston, A.B. (2019) Biochemical reconstruction of a metabolic pathway from a marine bacterium reveals its mechanism of pectin depolymerization. *Appl Environ Microbiol* **85**: e02114–e02118.

Hsieh, T.C., Ma, K.H., and Chao, A. (2016) iNEXT: an R package for rarefaction and extrapolation of species diversity (Hill numbers). *Methods Ecol Evol* **7**: 1451–1456.

Hu, F., Zhu, B., Li, Q., Yin, H., Sun, Y., Yao, Z., and Ming, D. (2019) Elucidation of a unique pattern and the role of carbohydrate binding module of an alginate lyase. *Mar Drugs* **18**: 32.

Ivanova, E., Ng, H.J., and Webb, H.K. (2014) The family *Pseudoalteromonadaceae*. In *The Prokaryotes*. Berlin: Springer.

Johnson, W.M., Alexander, H., Bier, R.L., Miller, D.R., Muscarella, M.E., Pitz, K.J., and Smith, H. (2020) Auxotrophic interactions: a stabilizing attribute of aquatic microbial communities? *FEMS Microbiol Ecol* **96**: fiaa115.

Kaberdin, V.R., Montánchez, I., Parada, C., Orruño, M., Arana, I., and Barcina, I. (2015) Unveiling the metabolic pathways associated with the adaptive reduction of cell size during *Vibrio harveyi* persistence in seawater microcosms. *Microb Ecol* **70**: 689–700.

Kabisch, A., Otto, A., König, S., Becher, D., Albrecht, D., Schüler, M., *et al*. (2014) Functional characterization of polysaccharide utilization loci in the marine *Bacteroidetes* '*Gramella forsetii*' KT0803. *ISME J* **8**: 1492–1502.

Kanehisa, M., and Sato, Y. (2020) KEGG mapper for inferring cellular functions from protein sequences. *Protein Sci* **29**: 28–35.

Kang, D.D., Li, F., Kirton, E., Thomas, A., Egan, R., An, H., and Wang, Z. (2019) MetaBAT 2: an adaptive binning algorithm for robust and efficient genome reconstruction from metagenome assemblies. *PeerJ* **7**: e7359.

Kappelmann, L., Krüger, K., Hehemann, J.-H., Harder, J., Markert, S., Unfried, F., *et al*. (2019) Polysaccharide utilization loci of North Sea *Flavobacteriia* as basis for using SusC/D-protein expression for predicting major phytoplankton glycans. *ISME J* **13**: 76–91.

Karst, S.M., Kirkegaard, R.H., and Albertsen, M. (2016) mmgenome: a toolbox for reproducible genome extraction from metagenomes. *bioRxiv* **059121**.

Katoh, K., Misawa, K., Kuma, K., and Miyata, T. (2002) MAFFT: a novel method for rapid multiple sequence alignment based on fast Fourier transform. *Nucleic Acids Res* **30**: 3059–3066.

Klippel, B., Lochner, A., Bruce, D.C., Davenport, K.W., Detter, C., Goodwin, L.A., *et al*. (2011) Complete genome sequence of the marine cellulose- and xylan-degrading bacterium *Glaciecola* sp. strain 4H-3-7+YE-5. *J Bacteriol* **193**: 4547–4548.

© 2021 The Authors. *Environmental Microbiology* published by Society for Applied Microbiology and John Wiley & Sons Ltd.,

Koch, H., Dürwald, A., Schweder, T., Noriega-Ortega, B., Vidal-Melgosa, S., Hehemann, J.-H., *et al*. (2019a) Biphasic cellular adaptations and ecological implications of *Alteromonas macleodii* degrading a mixture of algal polysaccharides. *ISME J* **13**: 92–103.

Koch, H., Freese, H.M., Hahnke, R., Simon, M., and Wietz, M. (2019b) Adaptations of *Alteromonas* sp. 76-1 to polysaccharide degradation: a CAZyme plasmid for ulvan degradation and two alginolytic systems. *Front Microbiol* **10**: 504.

Koch, H., Germscheid, N., Freese, H.M., Noriega-Ortega, B., Lücking, D., Berger, M., *et al*. (2020) Genomic, metabolic and phenotypic variability shapes ecological differentiation and intraspecies interactions of *Alteromonas macleodii*. *Sci Rep* **10**: 809.

Koedooder, C., Guéneuguès, A., Van Geersdaële, R., Vergé, V., Bouget, F.-Y., Labreuche, Y., *et al*. (2018) The role of the glyoxylate shunt in the acclimation to iron limitation in marine heterotrophic bacteria. *Front Mar Sci* **5**: 435.

Köseoğlu, V.K., Heiss, C., Azadi, P., Topchiy, E., Güvener, Z.T., Lehmann, T.E., *et al*. (2015) *Listeria monocytogenes* exopolysaccharide: origin, structure, biosynthetic machinery and c-di-GMP-dependent regulation. *Mol Microbiol* **96**: 728–743.

Krüger, K., Chafee, M., Ben Francis, T., Glavina del Rio, T., Becher, D., Schweder, T., *et al*. (2019) In marine *Bacteroidetes* the bulk of glycan degradation during algae blooms is mediated by few clades using a restricted set of genes. *ISME J* **13**: 2800–2816.

Lawlor, J. (2020) PNWColors. https://github.com/jakelawlor/PNWColors

Lee, J., Sperandio, V., Frantz, D.E., Longgood, J., Camilli, A., Phillips, M.A., and Michael, A.J. (2009) An alternative polyamine biosynthetic pathway is widespread in bacteria and essential for biofilm formation in *Vibrio cholerae*. *J Biol Chem* **284**: 9899–9907.

Li, H. (2018) Minimap2: pairwise alignment for nucleotide sequences. *Bioinformatics* **34**: 3094–3100.

Lombard, V., Golaconda Ramulu, H., Drula, E., Coutinho, P. M., and Henrissat, B. (2014) The carbohydrate-active enzymes database (CAZy) in 2013. *Nucleic Acids Res* **42**: D490–D495.

Love, M.I., Huber, W., and Anders, S. (2014) Moderated estimation of fold change and dispersion for RNA-seq data with DESeq2. *Genome Biol* **15**: 550.

Luis, A.S., Briggs, J., Zhang, X., Farnell, B., Ndeh, D., Labourel, A., *et al*. (2018) Dietary pectic glycans are degraded by coordinated enzyme pathways in human colonic *Bacteroides*. *Nat Microbiol* **3**: 210–219.

Mabeau, S., and Kloareg, B. (1987) Isolation and analysis of the cell walls of brown algae: *Fucus spiralis*, *F. ceranoides*, *F. vesiculosus*, *F. serratus*, *Bifurcaria bifurcata* and *Laminaria digitata*. *J Exp Bot* **38**: 1573–1580.

Martin, M. (2011) Cutadapt removes adapter sequences from high-throughput sequencing reads. *EMBnetjournal* **17**: 10–12.

Martin, M., Barbeyron, T., Martin, R., Portetelle, D., Michel, G., and Vandenbol, M. (2015) The cultivable surface microbiota of the brown alga *Ascophyllum nodosum* is enriched in macroalgal-polysaccharide-degrading bacteria. *Front Microbiol* **6**: 1487.

McMurdie, P.J., and Holmes, S. (2013) Phyloseq: An R package for reproducible interactive analysis and graphics of microbiome census data. *PLoS One* **8**: e61217.

Miller, M.A., Pfeiffer, W., and Schwartz, T. (2010) Creating the CIPRES science gateway for inference of large phylogenetic trees. Proceedings of the Gateway Computing Environments Workshop, pp. 1–8.

Mitulla, M., Dinasquet, J., Guillemette, R., Simon, M., Azam, F., and Wietz, M. (2016) Response of bacterial communities from California coastal waters to alginate particles and an alginolytic *Alteromonas macleodii* strain. *Environ Microbiol* **18**: 4369–4377.

Moriya, Y., Itoh, M., Okuda, S., Yoshizawa, A.C., and Kanehisa, M. (2007) KAAS: an automatic genome annotation and pathway reconstruction server. *Nucleic Acids Res* **35**: W182–W185.

Mühlenbruch, M., Grossart, H.-P., Eigemann, F., and Voss, M. (2018) Mini-review: phytoplankton-derived polysaccharides in the marine environment and their interactions with heterotrophic bacteria. *Environ Microbiol* **20**: 2671–2685.

Na, S.-I., Kim, Y.O., Yoon, S.-H., Ha, S., Baek, I., and Chun, J. (2018) UBCG: up-to-date bacterial core gene set and pipeline for phylogenomic tree reconstruction. *J Microbiol* **56**: 281–285.

Ndeh, D., Munoz, J.M., Cartmell, A., Bulmer, D., Wills, C., Henrissat, B., and Gray, J. (2018) The human gut microbe *Bacteroides thetaiotaomicron* encodes the founding member of a novel glycosaminoglycan-degrading polysaccharide lyase family PL29. *J Biol Chem* **293**: 17906–17916.

Neumann, A.M., Balmonte, J.P., Berger, M., Giebel, H.A., Arnosti, C., Brinkhoff, T., *et al*. (2015) Different utilization of alginate and other algal polysaccharides by marine *Alteromonas macleodii* ecotypes. *Environ Microbiol* **17**: 3857–3868.

Palovaara, J., Akram, N., Baltar, F., Bunse, C., Forsberg, J., Pedrós-Alió, C., *et al*. (2014) Stimulation of growth by proteorhodopsin phototrophy involves regulation of central metabolic pathways in marine planktonic bacteria. *Proc Natl Acad Sci U S A* **111**: E3650–E3658.

Parks, D.H., Imelfort, M., Skennerton, C.T., Hugenholtz, P., and Tyson, G.W. (2015) CheckM: assessing the quality of microbial genomes recovered from isolates, single cells, and metagenomes. *Genome Res* **25**: 1043–1055.

Pedler, B.E., Aluwihare, L.I., and Azam, F. (2014) Single bacterial strain capable of significant contribution to carbon cycling in the surface ocean. *Proc Natl Acad Sci U S A* **111**: 7202–7207.

Poghosyan, L., Koch, H., Frank, J., van Kessel, M.A.H.J., Cremers, G., van Alen, T., *et al*. (2020) Metagenomic profiling of ammonia- and methane-oxidizing microorganisms in two sequential rapid sand filters. *Water Res* **185**: 116288.

Quast, C., Pruesse, E., Yilmaz, P., Gerken, J., Schweer, T., Yarza, P., *et al*. (2013) The SILVA ribosomal RNA gene database project: improved data processing and web-based tools. *Nucleic Acids Res* **41**: D590–D596.

Rodriguez-R, L.M., Gunturu, S., Harvey, W.T., Rosselló-Mora, R., Tiedje, J.M., Cole, J.R., and Konstantinidis, K.T.

© 2021 The Authors. *Environmental Microbiology* published by Society for Applied Microbiology and John Wiley & Sons Ltd.,

(2018) The microbial genomes atlas (MiGA) webserver: taxonomic and gene diversity analysis of *Archaea and Bacteria* at the whole genome level. *Nucleic Acids Res* **46**: W282–W288.

Rodriguez-R, L.M., and Konstantinidis, K.T. (2016) The enveomics collection: a toolbox for specialized analyses of microbial genomes and metagenomes. *PeerJ Preprints*: **4**: e1900v1.

Roux, F.L., Zouine, M., Chakroun, N., Binesse, J., Saulnier, D., Bouchier, C., *et al*. (2009) Genome sequence of *Vibrio splendidus*: an abundant planctonic marine species with a large genotypic diversity. *Environ Microbiol* **11**: 1959–1970.

Saier, M.H., Reddy, V.S., Tsu, B.V., Ahmed, M.S., Li, C., and Moreno-Hagelsieb, G. (2016) The transporter classification database (TCDB): recent advances. *Nucleic Acids Res* **44**: D372–D379.

Salazar, G., Paoli, L., Alberti, A., Huerta-Cepas, J., Ruscheweyh, H.-J., Cuenca, M., *et al*. (2019) Gene expression changes and community turnover differentially shape the global ocean metatranscriptome. *Cell* **179**: 1068–1083.e21.

Satinsky, B.M., Zielinski, B.L., Doherty, M., Smith, C.B., Sharma, S., Paul, J.H., *et al*. (2014) The Amazon continuum dataset: quantitative metagenomic and metatranscriptomic inventories of the Amazon River plume, June 2010. *Microbiome* **2**: 17.

Schneider, D., Wemheuer, F., Pfeiffer, B., and Wemheuer, B. (2017) Extraction of total DNA and RNA from marine filter samples and generation of a cDNA as universal template for marker gene studies. **Methods Mol Biol 1539**: 13–22.

Schultz-Johansen, M., Bech, P.K., Hennessy, R.C., Glaring, M.A., Barbeyron, T., Czjzek, M., and Stougaard, P. (2018) A novel enzyme portfolio for red algal polysaccharide degradation in the marine bacterium *Paraglaciecola hydrolytica* S66^T encoded in a sizeable polysaccharide utilization locus. *Front Microbiol* **9**: 839.

Seemann, T. (2014) Prokka: rapid prokaryotic genome annotation. *Bioinformatics* **30**: 2068–2069.

Serafini, A., Tan, L., Horswell, S., Howell, S., Greenwood, D. J., Hunt, D.M., *et al*. (2019) *Mycobacterium tuberculosis* requires glyoxylate shunt and reverse methylcitrate cycle for lactate and pyruvate metabolism. *Mol Microbiol* **112**: 1284–1307.

Sim, P.-F., Furusawa, G., and Teh, A.-H. (2017) Functional and structural studies of a multidomain alginate lyase from *Persicobacter* sp. CCB-QB2. *Sci Rep* **7**: 13656.

Sivadon, P., Barnier, C., Urios, L., and Grimaud, R. (2019) Biofilm formation as a microbial strategy to assimilate particulate substrates. *Environ Microbiol Rep* **11**: 749–764.

Sperling, M., Piontek, J., Engel, A., Wiltshire, K.H., Niggemann, J., Gerdts, G., and Wichels, A. (2017) Combined carbohydrates support rich communities of particle-associated marine Bacterioplankton. *Front Microbiol* **8**: 65.

Spring, S., Scheuner, C., Göker, M., and Klenk, H.-P. (2015) A taxonomic framework for emerging groups of ecologically important marine gammaproteobacteria based on the reconstruction of evolutionary relationships using genome-scale data. *Front Microbiol* **6**: 281.

Stamatakis, A. (2014) RAxML version 8: a tool for phylogenetic analysis and post-analysis of large phylogenies. *Bioinformatics* **30**: 1312–1313.

Stocker, R. (2012) Marine microbes see a sea of gradients. *Science* **338**: 628–633.

Sun, X., Shen, W., Gao, Y., Cai, M., Zhou, M., and Zhang, Y. (2019) Heterologous expression and purification of a marine alginate lyase in *Escherichia coli*. *Protein Expr Purif* **153**: 97–104.

Sundberg, C., Al-Soud, W.A., Larsson, M., Alm, E., Yekta, S. S., Svensson, B.H., *et al*. (2013) 454 pyrosequencing analyses of bacterial and archaeal richness in 21 full-scale biogas digesters. *FEMS Microbiol Ecol* **85**: 612–626.

Teeling, H., Fuchs, B.M., Becher, D., Klockow, C., Gardebrecht, A., Bennke, C.M., *et al*. (2012) Substrate-controlled succession of marine bacterioplankton populations induced by a phytoplankton bloom. *Science* **336**: 608–611.

Teeling, H., Fuchs, B.M., Bennke, C.M., Krüger, K., Chafee, M., Kappelmann, L., *et al*. (2016) Recurring patterns in bacterioplankton dynamics during coastal spring algae blooms. *eLife* **5**: e11888.

Thomas, F., Lundqvist, L.C.E., Jam, M., Jeudy, A., Barbeyron, T., Sandström, C., *et al*. (2013) Comparative characterization of two marine alginate lyases from *Zobellia galactanivorans* reveals distinct modes of action and exquisite adaptation to their natural substrate. *J Biol Chem* **288**: 23021–23037.

Uhl, F., Bartsch, I., and Oppelt, N. (2016) Submerged kelp detection with hyperspectral data. *Remote Sens* **8**: 487.

van Bodegom, P. (2007) Microbial maintenance: a critical review on its quantification. *Microb Ecol* **53**: 513–523.

Van Truong, L., Tuyen, H., Helmke, E., Binh, L.T., and Schweder, T. (2001) Cloning of two pectate lyase genes from the marine Antarctic bacterium *Pseudoalteromonas haloplanktis* strain ANT/505 and characterization of the enzymes. *Extremophiles* **5**: 35–44.

Verdugo, P. (2012) Marine microgels. *Ann Rev Mar Sci* **4**: 375–400.

Verdugo, P., Alldredge, A.L., Azam, F., Kirchman, D.L., Passow, U., and Santschi, P.H. (2004) The oceanic gel phase: a bridge in the DOM–POM continuum. *Mar Chem* **92**: 67–85.

Vetter, Y.A., Deming, J.W., Jumars, P.A., and Krieger-Brockett, B.B. (1998) A predictive model of bacterial foraging by means of freely released extracellular enzymes. *Microb Ecol* **36**: 75–92.

Warnes, G., Bolker, B., and Lumley, T. (2020). gtools package. https://rdrr.io/cran/gtools/

Wickham, H., Averick, M., Bryan, J., Chang, W., McGowan, L.D., François, R., *et al*. (2019) Welcome to the Tidyverse. *J Open Source Softw* **4**: 1686.

Wolter, L.A., Mitulla, M., Kalem, J., Daniel, R., Simon, M., and Wietz, M. (2021b) CAZymes in *Maribacter dokdonensis* 62-1 from the Patagonian shelf: genomics and physiology compared to related flavobacteria and a co-occurring *Alteromonas* strain. *Front Microbiol* **12**: 628055.

Wolter, L.A., Wietz, M., Ziesche, L., Breider, S., Leinberger, J., Poehlein, A., *et al*. (2021a) *Pseudooceanicola algae* sp. nov., isolated from the marine macroalga *Fucus spiralis*, shows genomic and physiological adaptations for an algae-associated lifestyle. *Syst Appl Microbiol* **44**: 126166.

© 2021 The Authors. *Environmental Microbiology* published by Society for Applied Microbiology and John Wiley & Sons Ltd.,

Zäncker, B., Engel, A., and Cunliffe, M. (2019) Bacterial communities associated with individual transparent exopolymer particles (TEP). *J Plankton Res* **41**: 561–565.

Zhang, H., Yohe, T., Huang, L., Entwistle, S., Wu, P., Yang, Z., *et al*. (2018) dbCAN2: a meta server for automated carbohydrate-active enzyme annotation. *Nucleic Acids Res* **46**: W95–W101.

Zhu, Y., Chen, P., Bao, Y., Men, Y., Zeng, Y., Yang, J., *et al*. (2016) Complete genome sequence and transcriptomic analysis of a novel marine strain *Bacillus weihaiensis* reveals the mechanism of brown algae degradation. *Sci Rep* **6**: 38248.

Zhu, Y., Thomas, F., Larocque, R., Li, N., Duffieux, D., Cladière, L., *et al*. (2017) Genetic analyses unravel the crucial role of a horizontally acquired alginate lyase for brown algal biomass degradation by *Zobellia galactanivorans*. *Environ Microbiol* **19**: 2164–2181.

Supporting Information

Additional Supporting Information may be found in the online version of this article at the publisher's web-site:

Supplementary Fig. 1. A. Sampling location (cross) near Helgoland Island above dense macroalgal forests; schematically depicted in green. B. Conceptual overview of experimental setup using custom polysaccharide particles (insert). Magnetic particles were separated from their non-magnetic counterparts by magnetic selection (Supplementary Video 1) and frozen in cryotubes. FL communities were sampled by size-fractionated filtration of the supernatant (5 μm followed by 0.2 μm). Ambient seawater (start) and control samples (CTR) were directly filtered on 0.2 μm. Amplicon (0, 24, 48 and 60 h), metagenomic (24 and 60 h), and metatranscriptomic sequence data (60 h) were generated after different intervals of incubation.

Supplementary Fig. 2. Relative abundances of bacterial genera (top) and inverse Simpson alpha-diversity index (bottom) on alginate (AlgP) and pectin particles (PecP), in the free-living fraction (FL), control incubations (CTR) and the ambient *in situ* community (start). Only genera with abundances >4% are shown.

Supplementary Fig. 3. Relative abundances of *Colwellia* and *Glaciecola* ASVs in PA and FL communities. Each colour corresponds to a distinct ASV.

Supplementary Fig. 4. Maximum-likelihood phylogeny of MAGs based on 92 single-copy core genes, including the five near-complete MAGs (>90% completeness, <10% contamination), medium-quality MAGs (>70% completeness, <10% contamination) assigned to the same genus, and other related genomes.

Supplementary Fig. 5. Degradation of alginate and pectin based on Hobbs *et al*., 2019 and Koch *et al*., 2019a. TBDR: TonB-dependent receptor; MFS: major facilitator superfamily transporter; TRAP: tripartite ATP-independent transporter; DehR: DEH reductase; KdgK: KDG kinase; KdgA: KDGP aldolase; KdgF: responsible for uronate linearisation; KduI: 4-deoxy-L-threo-5-hexosulose-uronate ketol-isomerase; KduD: 2-deoxy-D-gluconate 3-dehydrogenase; UxaA: altronate dehydratase; UxaB: fructuronate reductase; UxaC: glucuronate isomerase; DEH: 4-deoxy-L-erythro-5-hexoseulose uronate; KDG: 2-keto-3-deoxy-D-gluconate; KDGP 2-keto-3-deoxy-6-phosphogluconate.

Supplementary Fig. 6. Detailed architecture of PUL in MAGs.

Supplementary Fig. 7. A: Truncated alginolytic operon in *Glaciecola*-MAG Gla-32 compared to the functionally characterized PUL in *Alteromonas macleodii* 83–1. BLASTp confirmed that missing genes were not encoded on other Gla-32 contigs. B: Hybrid biosynthetic gene cluster in *Psychromonas*-MAG Psym-73 encoding a siderophore homologous to a functional cluster in *Alteromonas* sp. 76–1 (left section) as well as spermidine-related genes homologous to VC1623 and VC1624 in *Vibrio cholerae* (right section). Locus tags are shown inside the first and last gene.

Supplementary Fig. 8. Maximum-likelihood phylogeny of PL7 genes from *Psychromonas*-MAG Psym-73, using BAB03312.1 from *Sphingomonas* as outgroup. Only some homologues showed substantial transcript abundances (right insert).

Supplementary Fig. 9. Rarefaction and coverage analysis of amplicon reads.

Supplementary Table 1. Metadata, sampling strategy, and statistics from amplicon, metagenome and metatranscriptome sequencing.

Supplementary Table 2. Complete overview of metagenomic genes, their abundance in metatranscriptomes (transcripts per million), and their assignment to CAZyme and KEGG categories.

Supplementary Table 3. Complete overview of differential transcript abundance analysis.

Supplementary Table 4. Complete overview of metagenome-assembled genomes.

Supplementary Table 5. Comparison of *Tenacibaculum*-MAG Ten-26 and *Psychromonas*-MAG Psym-73 with *Psychromonas* sp. B3M02 and *Tenacibaculum* sp. E3R01 from Enke *et al*. 2019 (https://doi.org/10.1016/j.cub.2019.03.047).

Supplementary Table 6. Composition of alginate and pectin particles.

Supplementary Video 1. Magnetic polysaccharide particles.

© 2021 The Authors. *Environmental Microbiology* published by Society for Applied Microbiology and John Wiley & Sons Ltd.,